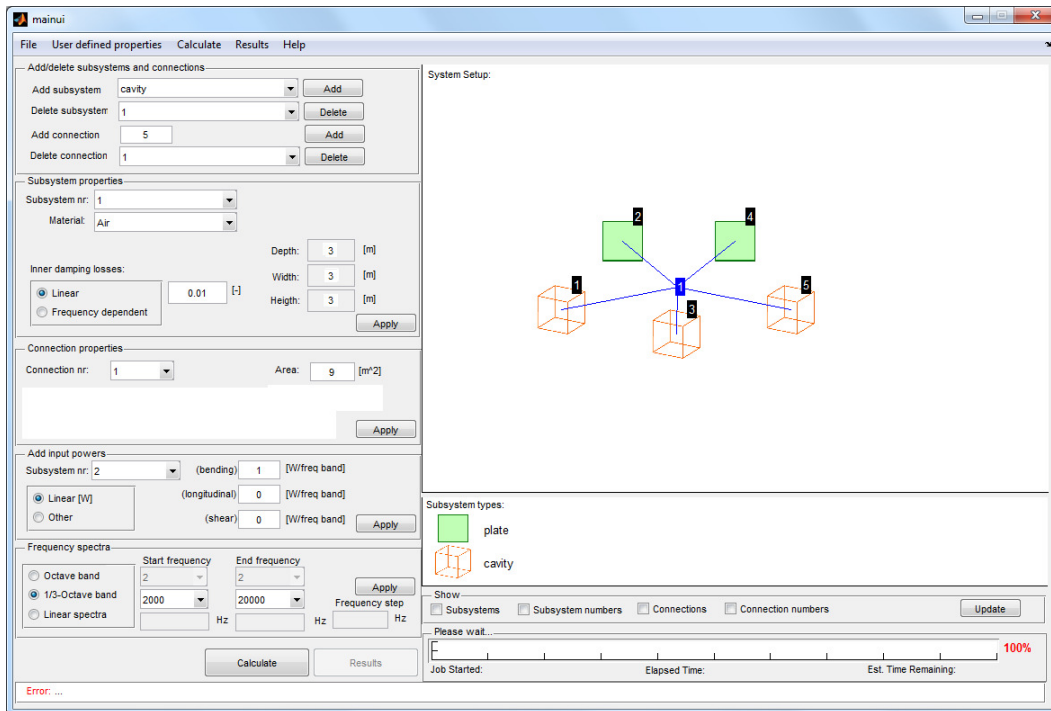


CHALMERS



Statistical Energy Analysis software

Development and implementation of an open source code
in Matlab/Octave

Master's Thesis in the Master's programme in Sound and Vibration

DANIEL JOHANSSON

PETER COMNELL

Department of Civil and Environmental Engineering

Division of Applied Acoustics

Vibroacoustics Group

CHALMERS UNIVERSITY OF TECHNOLOGY

Göteborg, Sweden 2010

Master's Thesis 2010:130

MASTER'S THESIS 2010:130

Statistical Energy Analysis software

Development and implementation of an open source code in Matlab/Octave

Master's Thesis in the Master's programme in Sound and Vibration

DANIEL JOHANSSON

PETER COMNELL

Department of Civil and Environmental Engineering

Division of Applied Acoustics

Vibroacoustics Group

CHALMERS UNIVERSITY OF TECHNOLOGY

Göteborg, Sweden 2010

Statistical Energy Analysis software
Development and implementation of an open source code in Matlab/Octave
Master's Thesis in the Master's programme in Sound and Vibration

DANIEL JOHANSSON

PETER COMNELL

© DANIEL JOHANSSON, PETER COMNELL 2010

Master's Thesis 2010:

Department of Civil and Environmental Engineering

Division of Applied Acoustics

Vibroacoustics Group

Chalmers University of Technology

SE-412 96 Göteborg

Sweden

Telephone: + 46 (0)31-772 1000

Cover:

Graphical user interface of the developed software, SEAlab, demonstrating a SEA model of a double leaf wall.

Chalmers reproservice
Göteborg, Sweden 2010

Statistical Energy Analysis software

Development and implementation of an open source code in Matlab/Octave

Master's Thesis in the Master's programme in Sound and Vibration

DANIEL JOHANSSON & PETER COMNELL

Department of Civil and Environmental Engineering

Division of Applied Acoustics

Vibroacoustics Group

Chalmers University of Technology

ABSTRACT

The available software for calculating Statistical Energy Analysis (SEA) is often written with closed source code. A user defines some input data for a system and will be presented with a result but with no information on how these results were calculated. The software acts like a "black box". There are usually also limited possibilities to modify specific alterations to these calculations. Therefore there is a need for software that is written in open source code which gives the user possibilities to modify calculation methods and provide a better understanding on how to interpret the results.

Another problem with today's SEA-calculation software are that they are often combined with other software into large packages which makes them quite expensive and may force the users to purchase software that are of no use for them. With open source code, the software will always be free of charge and available for anyone to use.

The aim of this Master's Thesis has been to construct a SEA-calculation software using open source code in Matlab, with the key component to design it in such a way that future developments can easily be made.

Focus in this thesis has been on implementing SEA-calculation methods for systems build up of isotropic plates connected via a line junction. Area connections are also implemented in order to calculate the sound transmission between rooms separated by single or double leaf walls. The method used to make this possible has been literature study and MATLAB programming.

Validations of the results are carried out by comparing three examples to a scientific article and a commercial software called AutoSEA v.1.5. The three examples are; two plates coupled together over a line junction, sound transmission through a single leaf wall and sound transmission through a double leaf wall.

Conclusions of the work is that the results correlates well with the article and the commercial software with the exception of the non-resonant transmission of the double leaf wall which needs to be further evaluated and validated.

Key words: statistical energy analysis, SEA, coupling loss factor, modal overlap, modal density, transmission coefficient, radiation efficiency, open source code

Contents

CONTENTS	I
PREFACE	III
NOTATIONS	IV
1 INTRODUCTION	1
1.1 Background	1
1.2 Aim	1
1.3 Goal	1
2 SOFTWARE SOURCE CODE	2
3 THEORY OF STATISTICAL ENERGY ANALYSIS	3
3.1 System definition	4
3.2 General SEA equations	5
3.3 Input power	7
3.4 Energy	9
3.5 Damping	9
3.6 Coupling loss factor	11
3.7 Modal density	14
3.8 Modal overlap	15
3.9 SEA assumptions and restrictions	16
3.9.1 Energy flow and modal energies	16
3.9.2 Strong and weak coupling	16
3.9.3 Modal overlap and number of modes	17
3.9.4 Uncorrelated sources	18
3.9.5 Conservative coupling	18
3.9.6 Maximum length	18
3.9.7 Maximum height	18
3.10 Material properties	19
4 CLF-COEFFICIENTS CALCULATION	20
4.1 Transmission coefficients	20
4.2 Radiation efficiency from finite plates	27
4.3 Non-resonant transmission	29
5 VALIDATION	31
5.1 Structural transmission coefficients	31

5.2	Single leaf wall	40
5.3	Double leaf wall example	45
6	DISCUSSION	51
7	CONCLUSION	54
7.1	Further work	55
8	REFERENCES	56
	APPENDIX A – DATA AND FOLDER STRUCTURE	57
	APPENDIX B – USER GUIDE	71

Preface

This thesis work has been carried out during spring and autumn of 2010 as a part of the finalization of the masters program at the Division of Applied Acoustics at the Chalmers University of technology in Gothenburg, Sweden. The basis of this work mostly consists of literature study and programming in Matlab.

We would like to take the opportunity to thank the people who in some way contributed to the work.

First of all we would like to thank our supervisor at Chalmers; Patrik Andersson for his useful input and willingness to help us. We would also like to thank our supervisors from A2Zound; Lars Ivarsson and Henrik Marberg for their constructive input and discussion of the software layout and handling and a special thanks to Lars whose idea it was to start this project. The willingness of Jens Forssén to take the time to answer our questions has been much appreciated. Also the technical help from Börje Wijk was of high value to us and saved us a lot of time.

Göteborg September 2010

Daniel Johansson

Peter Connell

Notations

Roman upper case letters

A	Total absorption
B	Bending stiffness
E	Energy
E_y	Young's modulus
F	Force (N)
K	Spring stiffness of cavity (N/m)
L	Length of the line connection (m)
L'	Length of perimeter (m)
M^F	Traction force according to Figure 4.2
N^F	Traction force according to Figure 4.2
P	Power
Q	Volume velocity (m^3/s)
R	Reduction index
R_{rad}	Radiation resistance
S	Surface area (m^2)
S'	Surface area of a volume (m^2)
S^F	Traction force according to Figure 4.2
T_{60}	Reverberation time (s)
T^F	Traction force according to Figure 4.2
V	Volume (m^3)
Y	Mobility
Z	Impedance

Roman lower case letters

c_0	Wave speed in fluid (m/s)
c_g	Group speed (m/s)
d	Cavity width (m)
f	Frequency (Hz)
f_c	Critical frequency (Hz)
f_{11}	First mode shape (Hz)
f_{dw}	Double leaf wall resonance frequency (Hz)

f_d	Cavity stops acting like a spring with constant stiffness (Hz)
h	Height (m)
k	Wave number
l	Length (m), $l_1 \geq l_2$
m	Mass (kg)
n	Modal density
p	Pressure (Pa)
t	Time (s)
u^d	Displacement according to Figure 4.2
v	Velocity (m/s)
v^d	Displacement according to Figure 4.2
w^d	Displacement according to Figure 4.2

Greek lower case letters

α	Wave amplitude
α'	Absorption coefficient
η	Loss factor
η_{ij}	Coupling loss factor, from subsystem i to j .
η_i	Total loss factor for subsystem i .
η_{id}	Internal loss factor for subsystem i .
θ	Plate-Plate junction angle
θ^d	Displacement according to Figure 4.2
ϑ	Poissons ration.
λ	Wave length (m)
ρ	Mass per unit area (kg/m^2)
ρ_0	Density of fluid (kg/m^3)
σ	Radiation efficiency
τ	Transmission coefficient
ϕ	Incident wave angle
ω	Angular frequency

Vectors & Matrixes

K Dynamic stiffness matrix

R Geometrical matrix

F Force vector

a Displacement vector

b Displacement vector

f Dynamic load vector

Acronyms

CLF Coupling Loss Factor

SEA Statistical Energy Analysis

1 Introduction

Statistical energy analysis has been used as an estimation technique for mid and high frequency vibration and sound transmission since it first arose in the mid 1960's. SEA, short for Statistical energy analysis, has since then proven successful and has today a wide application range, stretching from buildings to spacecraft.

1.1 Background

The available software for calculating SEA often has closed source code which means that the user does not know how the software calculates the results, the software acts like a "black box" e.g. the user loads input data and the software returns results and everything in-between remains hidden from the user.

Another incitement for this thesis is that the commercial SEA software is often combined with other software into larger packages. The license for such a package is often expensive and may come with software that are of no use to the user.

1.2 Aim

The aim of this master thesis is to construct and implement an SEA-calculation software. The software, called SEALab, should be written in Matlab and the programming should be well documented and open for the user. SEALab should be designed in such a way that future modifications could easily be made. As a start the software should be able to handle isotropic plate transmission and sound transmission between rooms separated by a wall constructed by single or double leaves.

1.3 Goal

The goal is to construct a user-friendly Matlab program that conducts SEA calculations. The software should be constructed in such a way that it could easily be modified to the user's specifications. This will be fulfilled by the use of functions in the program. Functions can easily be overviewed and modified. The use of functions enables the user to create new function that can be integrated in the software.

2 Software source code

All software has a source code. Usually the source code is open or closed to the user, meaning if the user has access to the source code or not. There are many different types of licenses that regulate the user insight and modification capabilities in the software. The source code in SEAlab is open for everyone and is regulated by the BSD license: [11]

Copyright (c) 2010, Daniel Johansson & Peter Connell
All rights reserved.

- Redistribution and use in source and binary forms, with or without modification, are permitted provided that the following conditions are met:
- Redistributions of source code must retain the above copyright notice, this list of conditions and the following disclaimer.
- Redistributions in binary form must reproduce the above copyright notice, this list of conditions and the following disclaimer in the documentation and/or other materials provided with the distribution.
- Neither the name of the technical university of Chalmers, Gothenburg nor the names of its contributors may be used to endorse or promote products derived from this software without specific prior written permission.

THIS SOFTWARE IS PROVIDED BY THE COPYRIGHT HOLDERS AND CONTRIBUTORS "AS IS" AND ANY EXPRESS OR IMPLIED WARRANTIES, INCLUDING, BUT NOT LIMITED TO, THE IMPLIED WARRANTIES OF MERCHANTABILITY AND FITNESS FOR A PARTICULAR PURPOSE ARE DISCLAIMED. IN NO EVENT SHALL THE COPYRIGHT HOLDER OR CONTRIBUTORS BE LIABLE FOR ANY DIRECT, INDIRECT, INCIDENTAL, SPECIAL, EXEMPLARY, OR CONSEQUENTIAL DAMAGES (INCLUDING, BUT NOT LIMITED TO, PROCUREMENT OF SUBSTITUTE GOODS OR SERVICES; LOSS OF USE, DATA, OR PROFITS; OR BUSINESS INTERRUPTION) HOWEVER CAUSED AND ON ANY THEORY OF LIABILITY, WHETHER IN CONTRACT, STRICT LIABILITY, OR TORT (INCLUDING NEGLIGENCE OR OTHERWISE) ARISING IN ANY WAY OUT OF THE USE OF THIS SOFTWARE, EVEN IF ADVISED OF THE POSSIBILITY OF SUCH DAMAGE.

The advantage with an open source code is that the user can inspect the code and see exactly how the software processes the input data. Open source also makes it easier for the user to modify and create own applications to the software according to his/hers specifications.

Matlab were chosen as the programming language because it is widely used and it is relatively cheap in comparison to SEA software. Also it is closely related to the free software Octave. Many of the important functions used in SEAlab works in an Octave environment.

3 Theory of Statistical Energy Analysis

Statistical Energy Analysis, or (SEA) is a structural-acoustic method that is widely used. SEA arose during the 1960's in the aerospace industry to predict the vibrational behavior when designing space craft. During this time computational methods were available but the size of the models that could be handled and the computational speed were such that only few of the lowest order modes could be predicted. [1] Furthermore, in traditional analysis of mechanical vibration the lowest modes are usually of most interest because these modes normally have the greatest displacement response. But when designing and constructing large and lightweight aerospace structures it is apparent that also high frequency broad-band loads is important in the process of predicting structural fatigue, equipment failure and noise production. [2] The development and use of SEA proved to be a good method to predict high frequency loads and the analysis technique has since then been applied, extended and developed for a growing number of applications. For example it has been used to model sound and vibration transmission in buildings, cars, aircrafts, ships and trains. [3]

The name SEA points out certain aspects of the method. *Statistical* accents that the system being considered are a member of a population of similar systems with known distributions of the subsystem parameters. *Energy* is the variable of interest. It describes the behavior of the system in terms of stored, dissipated and exchanged energies of vibration. Other often used variables for acoustic and structural vibration, such as displacement, pressure etc. can be derived from the energy of vibration. *Analysis* emphasizes that SEA is a framework rather than a specific technique. [2]

In order to model the exchange of vibrational energy within a system, it is crucial that the system is divided into several subsystems. SEA models the sound transmission in systems and energy distribution over the subsystems by power balance equations. Total incoming power on one hand and the total dissipated power on the other are equal.

In order to evaluate how the transferred power between the subsystems are related to their equilibrium energies, certain transmission coefficients needs to be evaluated. There are three main approaches to estimates these coefficients. These are the modal approach, the wave approach and the mobility approach. The modal approach governs the interaction of the uncoupled modes in the subsystems. With boundary conditions which express the decoupling it is possible to express the multimode power transfer coefficients. This approach is well suited for vibroacoustic problems involving acoustic interaction between enclosed volumes. The modal approach is not ideally suited to couplings between solid structures, this is where the second approach comes in handy, the wave approach. In this approach the vibrational fields are modeled as superposition of traveling waves and the transferred power between subsystems can be derived from wave transmission and reflections at the subsystem interfaces. The third approach is the mobility approach.

The mobility approach utilizes the concept of dynamic mobility, or impedance to express the interaction of the coupled subsystems.[1]

In this project the wave approach is utilized for coupling between structures, for couplings with volumes a standardized method reference [4] will be utilized. The main reason for this method is that it is commonly used among engineers and that it is a standardized method.

3.1 System definition

Sound transmission through for example a wall in a building is only represented by a limited part of the entire building, 'the system'. It is important that the model contain as much as possible of the influencing parts of the building to provide reliable results. However, not more than necessary should be treated in order to not make it too complex which increases the chance of errors and also larger computation times.

In SEA, each system is divided into several physical elements of a suitable size. These elements are divided so that the vibro-acoustic characteristics are similar over them, such as damping, excitation and coupling properties. These elements are called subsystems. For example, an isotropic plate is usually treated as three subsystems corresponding to the different wave types in the plate, (flexural, longitudinal and shear waves). Only wave types that play an important part in the transmission, dissipation and storage of energy need to be included as subsystems in a model. So for example in a fluid volume only longitudinal waves are important for the sound transmission and the fluid volume can therefore be treated as a single subsystem.

3.2 General SEA equations

The principles of SEA can be illustrated as shown in Figure 3.1 below. This system consists of two connected subsystems.

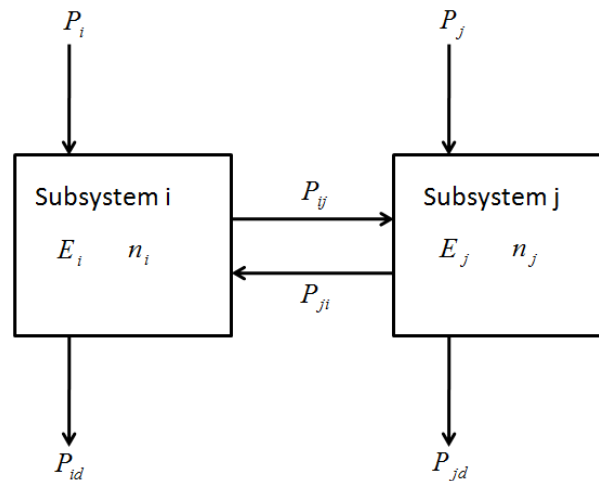


Figure 3.1 SEA model of two subsystems.

Energy flows in and out of a subsystem. The energy that flows out consist of dissipation (P_{id} and P_{jd}), radiation and transmission to other subsystems (P_{ij} or P_{ji}). The energy that flows into a subsystem consist of external source excitations (P_i and P_j) and transmissions from other subsystems (P_{ij} or P_{ji}).

The dissipated power in a subsystem is given by equation 3.1 below:

$$P_{id} = \omega \eta_{id} E_i \quad (3.1)$$

where η_{id} is referred to as the damping loss factor and E_i is the total vibrational energy of the modes at frequency f .

The net transmitted power between subsystem i and j (P_{ij}) is given by equation 3.2

$$P_{ij} = \omega \eta_{ij} E_i \quad (3.2)$$

SEA calculation is based on energy flow equilibrium. The power balances for the two systems are given as in equations 3.3 and 3.4

$$P_i + P_{ji} = P_{ij} + P_{id} \quad (3.3)$$

$$P_j + P_{ij} = P_{ji} + P_{jd} \quad (3.4)$$

When combining equations 3.1-3.4, the power balance equation for two subsystems can be expressed in matrix form shown in equation 3.5

$$\begin{bmatrix} P_i \\ P_j \end{bmatrix} = \omega \begin{bmatrix} (\eta_{id} + \eta_{ij}) & -\eta_{ji} \\ -\eta_{ij} & (\eta_{jd} + \eta_{ji}) \end{bmatrix} * \begin{bmatrix} E_i \\ E_j \end{bmatrix} \quad (3.5)$$

For a more generalized case with n number of subsystems, the balance equations can be written in a general form as, equation 3.6

$$\begin{bmatrix} P_i \\ P_j \\ \vdots \\ P_n \end{bmatrix} = \omega \begin{bmatrix} \eta_i & -\eta_{ji} & \dots & -\eta_{ni} \\ -\eta_{ij} & \eta_j & \ddots & \vdots \\ \vdots & \ddots & \ddots & \vdots \\ -\eta_{in} & \dots & \dots & \eta_n \end{bmatrix} * \begin{bmatrix} E_i \\ E_j \\ \vdots \\ E_n \end{bmatrix} \quad (3.6)$$

Where η_i equals the total loss factor and is the summation of the damping loss factor of the subsystem and the coupling loss factors representing energy transmission from the subsystem to others, equation 3.7.

$$\eta_i = \eta_{id} + \sum_{j=1, j \neq i}^n \eta_{ij} \quad (3.7)$$

The matrix can also be described in a symmetric form as in equation 3.8.

$$\begin{bmatrix} P_i \\ P_j \\ \vdots \\ P_n \end{bmatrix} = \omega \begin{bmatrix} \eta_i n_i & -\eta_{ji} n_j & \dots & -\eta_{ni} n_n \\ -\eta_{ij} n_i & \eta_j n_j & \ddots & \vdots \\ \vdots & \ddots & \ddots & \vdots \\ -\eta_{in} n_i & \dots & \dots & \eta_n n_n \end{bmatrix} * \begin{bmatrix} E_i/n_i \\ E_j/n_j \\ \vdots \\ E_n/n_n \end{bmatrix} \quad (3.8)$$

Where n is the modal density, further described in chapter 3.9. The general matrix and the symmetric is basically the same except that the energy is now described as the modal energy instead of energy as in the general matrix. The modal energy is defined as the energy in the subsystem divided by the modal density. The advantage of describing the matrix in a symmetric form is that the consistency relationship can be used. The consistency relationship states the relation between two subsystems modal energies and their coupling loss factors as shown in equation 3.9.

$$n_i \eta_{ij} = n_j \eta_{ji} \quad (3.9)$$

By using the consistency relationship only the coupling loss factors for one transmission direction are needed to calculate the energy exchange between two subsystems. This means that only the upper triangular or the lower triangular side of the symmetric matrix explained in equation 3.8 needs to be calculated, the rest can be calculated by the consistency relationship and thereby save a lot of numerical calculations. [3]

For most systems, especially large systems, many subsystems are not connected. This means that the matrix will contain many zero off-diagonal elements and therefore a sparse matrix. If the consistency relationship is applied, prediction tools can utilize this to lower the computation time and required memory usage. For SEA modeling these matrixes will for most systems still be relatively small compared to for example those used in FEM models and given the performance of today's computers, using the consistency relationship, will not greatly affect the calculation speed. For some systems that require much computation performance, the consistency relationship should if possibly still be used. An example of this is plates coupled over a line junction at a certain connection angle and averaged over many incident angles to create a diffuse sound field in the plate, this will be described in chapter 3.

3.3 Input power

There are different ways to excite the structure and depending on the source the energy input in the subsystem differs. The different types of input power can for example be: mechanical point excitation or an acoustic source.

These external sources inject energy into one or more subsystems of a system. These sources can be described as forces, moments, pressures or motions.

The mechanical point excitations can be described as a force source or velocity source as:

Force source:

$$P_i = \frac{|F(\omega)|^2 \Re\{Y(\omega)\}}{2} \quad (3.10)$$

Velocity source:

$$P_i = \frac{|v(\omega)|^2 \Re\{Z(\omega)\}}{2} \quad (3.11)$$

where F is the force, v is the velocity and $\Re\{Y\}$ is the real part of the point mobility and $\Re\{Z\}$ is the real part of the impedance.

The force F and velocity v are related by the point mobility and impedance according to:

$$v = YF \quad (3.12)$$

$$F = Zv \quad (3.13)$$

Depending on the excitation point the real part of the mobility can be calculated for a plate by the equations shown in the table below.

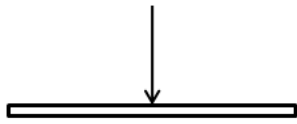
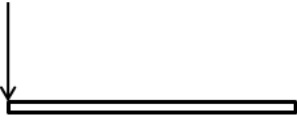
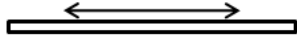
	$\Re\{Y\}$
	$\frac{1}{8\sqrt{B\rho}}$
	$\frac{1}{3.5\sqrt{B\rho}}$
	$\approx \frac{2\omega}{E_y h}$

Table 3.1 Different types of point excitations and their corresponding real part of the mobility

where B is the bending stiffness of a plate, ρ the mass per unit area, E the Young's modulus and h the thickness of the plate.

Acoustic sources usually have constant velocity, not constant power. The radiated power can be calculated by the equation

$$P_i = R_{rad}\overline{Q^2} \quad (3.14)$$

$\overline{Q^2}$ is the mean-square volume velocity and R_{rad} is the radiation resistance and can be calculated for a point source in free field as:

$$R_{rad} = \frac{\rho_0 c_0 k_0^2}{4\pi} \quad (3.15)$$

where ρ_0 , c_0 and k_0 are the density, wave speed and wave number in the free field respectively. [5]

3.4 Energy

As mentioned earlier the vibrational energy is the primary response variable of subsystems and it can be expressed in other acoustic variables that is more common, such as pressure and velocity.

For an acoustic subsystem i the energy is given by:

$$E_i = \frac{p_i^2 V_i}{\rho_i c_i^2} \quad (3.16)$$

p_i is the sound pressure (r.m.s.) averaged over the acoustic volume V_i . ρ_i and c_i are the density and the wave speed in the medium.

For a structural subsystem the Energy is given by:

$$E_i = m_i v_i^2 \quad (3.17)$$

where v_i is the velocity (r.m.s.) averaged over the surface area and m_i the total mass of the subsystem.

3.5 Damping

The damping loss factor of a subsystem can be described as:

$$\eta_{i,d} = \eta_{i,s} + \eta_{i,rad} + \eta_{i,b} \quad (3.18)$$

where:

$\eta_{i,s}$ is the loss factor for structural or material damping in the subsystem. This is basically the conversion from vibrations into heat.

$\eta_{i,rad}$ is the loss factor associated with acoustic radiation losses from the surface of the subsystem into the surrounding fluid medium. This can also be explained as the conversion of vibrations into sound. If the surrounding medium however is modeled as a subsystem in the system with its respective transmission coupling loss factor, this loss factor is not taken into account in the damping loss factor of subsystem i . The sound level caused in the room can then be predicted instead of just being included in the damping loss factor.

$\eta_{i,b}$ is the loss factor associated with coupling damping for subsystem i . This contribution can often be neglected in SEA modeling due to the assumption made that no energy is lost in the coupling. [12]

As mentioned before from equation 3.7 the total loss factor η_i can be described as the sum of all coupling loss factors from the subsystem to the other connected subsystems and the damping loss factor $\eta_{i,d}$ for the subsystem. This total loss factor is sometimes described to as the subsystem's damping.

There are several ways to estimate the total loss factor η_i for different types of subsystems without the need to calculate the damping loss factor or all the coupling loss factors to connecting subsystems. In building acoustics the most common way to calculate the total loss factor for a room is to use the reverberation time. The equation used to calculate the total loss factor then becomes:

$$\eta_i = \frac{2.2}{fT_{60}} \quad (3.19)$$

Where T_{60} is the reverberation time and is defined as the time it takes for the energy to decrease with 60dB from a steady state condition. The formula can be used for rooms as well as for structures but it can be difficult to measure the reverberation time in structures because of the short reverberation time. Large structures, like buildings, can be challenging to excite sufficiently.

The reverberation time can be calculated in rooms if the absorption of the room is known.

$$T_{60} = \frac{0.161V}{A} \quad (3.20)$$

Where A is the total absorption in a room and can be calculated as

$$A = \sum S\alpha' \quad (3.21)$$

Here S is the surface area that is multiplied with its corresponding absorption coefficient α' .

To estimate the total loss factor for a room when the reverberation time is unknown, a typical absorption A of $10m^2$ or a reverberation time T_{60} of 0.5 seconds can be used. [3]

When calculating the total loss factor for a cavity, as can be seen in double walls, the total loss is estimated by a different equation.

$$\eta_i = \frac{c_0 \sum l \alpha'}{2\pi f S} \quad (3.22)$$

Where l is the length multiplied with its corresponding absorption coefficient α' . A cavity is here defined as a room where the wave propagation is 2-dimensional. It is important to keep in mind that the value of the absorption coefficient α' differs if a material is placed in a cavity or a room. [3]

3.6 Coupling loss factor

The coupling loss factor is a parameter that is uniquely associated with SEA. It is possible to relate the coupling loss factors to other parameters that are used outside SEA such as radiation efficiency and transmission coefficients, which will be seen in the following equations in this chapter.

Coupling loss factors are used in SEA to describe the energy transmitted from one subsystem to another. The equations differ depending on the type of junction and the properties of the connected subsystems. The formulas presented below is the formulas used in the software and can be found in literature.

The coupling loss factor is defined as the fraction of energy that transmits from one subsystem to another. As described before the power transmitted from subsystem 1 to subsystem 2 for a general case can be described as:

$$P_{12} = E_1 \omega \eta_{12} \quad (3.23)$$

The energy E_1 in subsystem 1 can be described as mentioned before as:

$$E_1 = m_1 v_1^2 \quad (3.24)$$

Where m_1 is the mass and v_1 is the rms and spatial average of the velocity in subsystem 1. For a 2-dimensional subsystem, plates and cavities, equation 3.24 can be written as:

$$E_1 = \rho_1 S_1 v_1^2 \quad (3.25)$$

ρ_1 and S_1 are the density and surface area of subsystem 1. For a 3-dimensional subsystem, rooms, equation 3.24 can be described as:

$$E_1 = \rho_0 V_1 v_1^2 \quad (3.26)$$

Where ρ_0 is the fluid density and V_1 is the volume. Combining equations 3.23 and 3.25 provides the following expression for a 2-dimensional case.

$$P_{12} = \rho_1 S_1 v_1^2 \omega \eta_{12} \quad (3.27)$$

For two coupled plates the power transmission between the two plates can be described as

$$P_{trans} = P_{inc} \tau \quad (3.28)$$

Where τ is the transmission coefficient. Using the properties of a 2-dimensional diffuse field the incoming power can be described as

$$P_{inc} = \frac{E_1 c_{g1} L}{\pi S_1} = \frac{\rho_1 v_1^2 c_{g1} L}{\pi} \quad (3.29)$$

Here L is the length of the connection. Combining equations 3.27-3.29, the coupling loss factor for a plate-plate model can be described as:

$$\eta_{12} = \frac{L c_{g1} \tau_{12}}{\omega \pi S_1} \quad (3.30)$$

Where τ_{12} is the transmission coefficient between subsystem 1 and 2. c_g is the group speed and is calculated by the following equations for bending, longitudinal and shear waves. For bending waves the group speed is twice the phase speed c_b and is calculated as:

$$c_{g,b} = 2c_b = 2 \left(\frac{B\omega^2}{\rho} \right)^{1/4} \quad (3.31)$$

where B is the bending stiffness of the plate:

$$B = \frac{E_y h^3}{12(1-\nu^2)} \quad (3.32)$$

E_y is the Young's modulus, h is the thickness of the plate and ϑ is Poisson's ratio. For longitudinal and shear waves, the group speed is equal to the wave speed:

$$c_{g,l} = c_l = \sqrt{\frac{E_y h}{\rho(1-\vartheta^2)}} \quad (3.33)$$

$$c_{g,s} = c_s = \sqrt{\frac{E_y h}{2\rho(1-\vartheta)}} \quad (3.34)$$

When coupling a plate and a room, the coupling loss factor can be calculated in a similar way as for coupling two plates. Here the radiated power is defined as a fraction of the incoming wave as

$$P_{rad} = P_{plane} \sigma \quad (3.35)$$

Where σ is the radiation efficiency and P_{plane} is the radiated power of a flat surface generating a plane wave

$$P_{plane} = v_1^2 \rho_1 c_0 S_1 \quad (3.36)$$

ρ_1 , c_0 and S_1 are the mass per unit area, speed of sound and surface area. By setting equation 3.27 as the radiated power and combining it with equations 3.35-3.36 above one obtains

$$\eta_{12} = \frac{\rho_0 c_0 \sigma}{\omega \rho_1} \quad (3.37)$$

The non-resonant coupling loss factor for a room to another room or from a room to a cavity is defined as equation 3.28 but now the incoming power is described as

$$P_{inc} = \frac{E_1 c_0 S_1}{4V_1} \quad (3.38)$$

V_1 is the volume. Similar to coupling between two plates, equation 3.28 are combined with equation 3.38 and equation 3.26 to describe the coupling loss factor for room to room or room to cavity as:

$$\eta_{12} = \frac{c_0 S_1 \tau_{12}}{4\omega V_1} \quad (3.39)$$

The consistency relation, equation 3.9, is used with equation 3.39 to calculate the coupling loss factor from a cavity to a room.

3.7 Modal density

Modes is an essential part of SEA and occurs when the multiple of the wavelength of a subsystem and the dimensions of the subsystem match. When this happens the amplitude becomes larger due to constructive interference between waves travelling in the subsystem. Modes can also be referred to as resonances. The modes within a subsystem receive, store and transfer energy.

The modal density n_i of a subsystem is defined as the number of modes per unit frequency. As described in the beginning of this chapter the modal density is needed to calculate the symmetric matrix or the consistency relationship. If the coupling loss factors in both directions between all subsystems in a system are already known, the modal density is not needed for predictions in SEA using the general matrix form, Equation 3.6. The modal density is however useful to determine the suitability of the SEA model which will be described more in detail later in sections 3.8 and 3.9.3. To be able to calculate the modal energy rather than the total energy the modal density is also needed as explained in equation 3.8.

To derive the modal density of a subsystem, the geometrical information about the allowed mode shapes is combined with the dispersion relation for free waves in the subsystem.

For a 2-dimensional subsystem the modal density can be calculated from:

$$n(\omega) = \frac{Sk}{2\pi c_g} \quad (3.40)$$

For a 3-dimensional subsystem the equation to calculate the modal density will look like:

$$n(\omega) = \frac{1}{2\pi} \left(\frac{2\omega fV}{c_0^3} + \frac{\omega S'}{4c_0^2} + \frac{L'}{8c_0} \right) \quad (3.41)$$

S' is the total surface area, L' is the total length of all edges and V is the volume. These parameters can for a cubic volume be calculated as:

$$S' = 2(wd + dh + wh) \quad (3.42)$$

$$L' = 4(w + d + h) \quad (3.43)$$

Where w is the width, h the height and d the depth of the cubic volume.

An acoustic cavity behaves as a two dimensional subsystem depending on the frequency and depth of the cavity. The frequency used to determine whether the subsystem is two or three dimensional can be found below.

$$f = \frac{c_0}{2l} \quad (3.44)$$

Where c_0 is the speed of sound in the fluid and l is the depth of the cavity. Below the calculated frequency the subsystem acts like a two dimensional subsystem and above as a three dimensional subsystem.

The modal density can be used to calculate the number of modes in a specific frequency band which is used to calculate the energy per mode often referred to in SEA context. [3]

$$N = n(\omega)\Delta\omega \quad (3.45)$$

Where $\Delta\omega$ is the number of frequencies contained in the frequency band and n is the modal density.

3.8 Modal overlap

The modal overlap is closely related to the modal density and is defined as the ratio of the modal bandwidth to the average frequency spacing.

$$\text{Modal overlap} = \omega\eta_d n(\omega) \quad (3.46)$$

The modal bandwidth used in the formula can either be the half-power bandwidth, as above, or the effective bandwidth which is $\pi/2$ times the half-power bandwidth. [3] The modal overlap calculated with the effective bandwidth is sometimes referred to as the modal overlap factor. [6] The modal overlap factor is not a parameter that is used in predictions with SEA. It is however necessary to calculate the modal overlap to determine the suitability of the SEA model for the system which will be discussed in section 3.9.3.

3.9 SEA assumptions and restrictions

In this chapter the uncertainties and restriction of an SEA model is furthered described. There are several important requirements that need to be fulfilled for each subsystem in order for the assumptions used in SEA to be valid. The requirements should be seen as guidance more than absolute right or wrong. Depending on the demand of accuracy calculation can be made outside the requirements but then the uncertainties of the result accuracy increases.

3.9.1 Energy flow and modal energies

One assumption made for the SEA model to be accurate is that the flow of vibrational energy between two coupled subsystems is proportional to the subsystems difference in averaged coupled modal energies. This assumption can be assumed as valid for weakly coupled subsystems.

3.9.2 Strong and weak coupling

Strong and weak coupling is two extreme coupling cases that are important to know of. If a coupling is strong or weak depend on the relative sizes of the coupling to other subsystems and the internal damping. If two subsystems are considered, where subsystem 1 is being excited by the input power P_1 , then the energy in the two subsystems can be described as

$$E_1 = \frac{P_1}{\omega} \left(\frac{\eta_2 + \eta_{21}}{\eta_1 \eta_2 + \eta_2 \eta_{12} + \eta_1 \eta_{21}} \right) \quad (3.47)$$

$$E_2 = \frac{P_1}{\omega} \left(\frac{\eta_{12}}{\eta_1 \eta_2 + \eta_2 \eta_{12} + \eta_1 \eta_{21}} \right) \quad (3.48)$$

In the case of weak coupling the damping in both subsystems is much larger than the coupling between them e.g. $\eta_{21} \ll \eta_2$ and $\eta_{12} \ll \eta_1$. The energy equations then become.

$$E_1 \approx \frac{P_1}{\omega \eta_1} \quad (3.49)$$

$$E_2 \approx \frac{P_1 \eta_{12}}{\omega \eta_1 \eta_2} \quad (3.50)$$

The consequence of weak coupling is that almost all power dissipates in the excited subsystem and subsystem 2 does not affect subsystem 1.

Strong coupling is simply the opposite of weak coupling, the coupling is much larger than the internal damping, e.g. $\eta_{21} \gg \eta_2$ and $\eta_{12} \gg \eta_1$. The Energy equations for the two subsystems then become:

$$E_1 \approx \frac{P_1}{\omega(\eta_1 + \eta_2 n_2 / n_1)} \quad (3.51)$$

$$E_2 \approx \frac{P_1}{\omega(\eta_2 + \eta_1 n_1 / n_2)} \quad (3.52)$$

As can be seen in the equations above the energy in each subsystem no longer depend on the physical coupling between the subsystems.

SEA models are suitable when the coupling is assumed to be weak. How strict this requirement is are often discussed. SEA models with strong couplings have shown that there can be erroneous results as much as up to 30 dB for very similar system response or periodic systems, but for other cases it have shown to give reliable results. However, weak coupling condition should always be applied when choosing subsystems. [3], [5], [7]

3.9.3 Modal overlap and number of modes

The vibrational behavior of a highly damped subsystem is non-resonant which implies that SEA is not applicable. If the damping is not too high the larger a modal overlap and the larger number of modes in a frequency band will smooth the response spectra and the spatial variation in responses. This means that the results will be more reliable. So a minimum modal overlap and a minimum number of modes are required for the SEA model to be valid. Because the modal overlap is often larger at higher frequencies the modal overlap limit sets a lower frequency limit.

This lower frequency limit has been discussed by several authors. However, there will actually not be an exact frequency limit where the SEA model is not correct anymore for a minimum number of modes. The error will instead increase with decreasing frequency.

Even if it is never completely possible in practical solutions, one should try to choose subsystems in such a way that the modes and the energy over these modes within each subsystem are more or less evenly distributed over the frequency range of interest.

The number of modes alone is not sufficient to determine the accuracy of SEA, the damping of the modes is also important. The modal overlap is a more useful parameter to determine the validity of the SEA model.

According to reference [3] the modal overlap should be larger than unity e.g. 1 for the responses to be "damping controlled", which is an assumption in the SEA model.

Even though SEA is aimed for modeling resonant transmission between subsystems, non-resonant sound transmission can be integrated to some extent. This is further explained in chapter 4.3.

3.9.4 Uncorrelated sources

Another assumption made in SEA is that sources which excite the subsystems are not correlated. If the sources are uncorrelated the energies which originate from the individual sources can be summed linearly. It is desired that many modes in each frequency band considered are excited. From this point of view a broadband random excitation as a source is desirable.

3.9.5 Conservative coupling

There is linear, conservative coupling between subsystems. This means that there is no damping in the coupling. However, for some cases a very small coupling damping can still be integrated in the SEA model, it will then be implemented in the inner loss factor of the subsystems, see reference [12] for more information on this topic.

3.9.6 Maximum length

Due to damping of subsystems the amount of energy a wave carries travelling across the length of the subsystem decays. To prevent too much decay there is a need for a description of the maximum length a subsystem with a certain damping can have. Such a formula is described in ref [2] as:

$$l < \frac{c_g}{2\pi f \eta_d} \quad (3.53)$$

Where l is the maximum length of the subsystem, c_g is the groupspeed and η_d is the internal loss factor.

3.9.7 Maximum height

The so called Euler-Bernoulli models used for describing the behavior of plates state that the deformation of an element due to bending waves is much larger than for shear waves. Due to these assumptions there is a limit for using thin plate theory and is described as a relation between wavelength and thickness of the plate as described in the formula below. [8]:

$$\lambda > 6h \quad (3.54)$$

Where λ is the wavelength and h is the thickness of the plate. Note that this formula only concern bending waves.

3.10 Material properties

The material properties used in SEAlab are taken from reference [8].

Material	Density [kg/m ³]	E-modulus [10 ⁹ Pa]	Poisson's ratio
Steel	7800	210	0.3
Aluminum	2700	70	0.33
Glass	2500	60	-
Concrete	2300	36	0.2
Concrete (Autoclaved aerated)	1300	3.8	0.2
Concrete (Lightweight)	500	1.7	0.2
Gypsum plate	850	4.1	0.3
Chipboard	700	3.8	0.2

Table 3.2 Material properties used in SEAlab

4 CLF-coefficients calculation

In this chapter the needed coefficients will be described to be able to complete the calculations defined in the previous chapter. The three required parameters are the transmission coefficients, radiation efficiency and the non-resonant transmission.

4.1 Transmission coefficients

The equations used to calculate the transmission coefficients originate from the publication by Langley, see reference [9]. The analysis is based on the wave approach and concerns generic plate/beam junction with arbitrary number of semi-infinite plates, coupled through a beam or directly coupled to each other. Three types of waves are included; bending, longitudinal and shear.

Some modifications of the equations in Langley's paper were carried out in order to match software specification and to correct a couple of minor errors in reference [9]. In what follows, a short presentation and discussion of the equations will be performed. To reduce the amount of algebra a dynamic stiffness matrix approach is used. For further details of the analysis see reference [9].

The setup used in the Matlab code is a plate-plate coupling, see Figure 4.1 with the co-ordinate system shown in Figure 4.2 below.

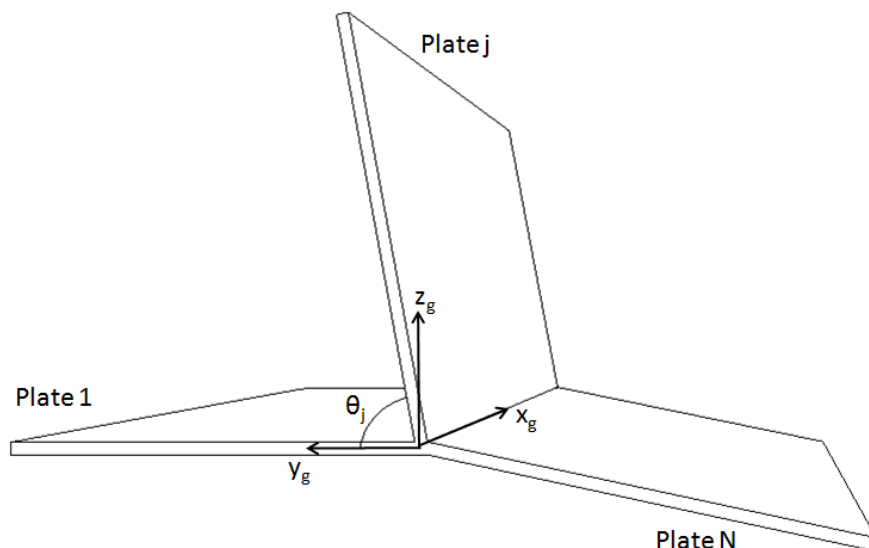


Figure 4.1 Plate-plate coupling with angles and co-ordinate system

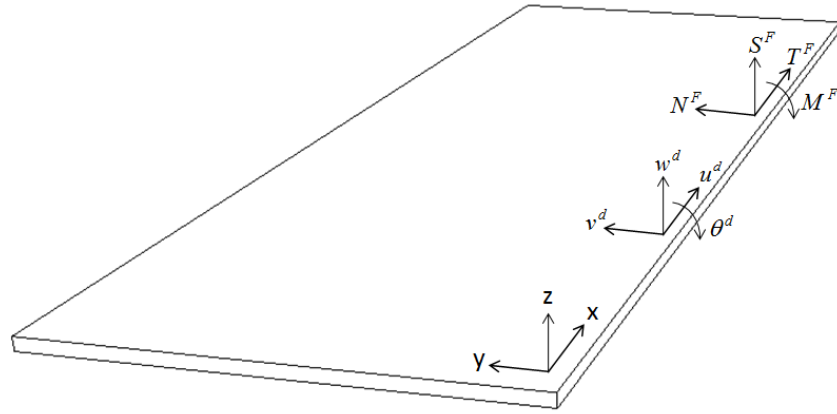


Figure 4.2 Displacement and traction co-ordinates

If a plane wave propagates towards the junction of the plate ensemble it has a space/time dependency, as in this case $e^{-ikx+i\mu y+i\omega t}$. Here x and y are the space coordinates and k and μ are the corresponding wavenumbers, ω is the angular frequency and t is the time. The continuity in the junction implies that all plates must have the dependency $e^{-ikx+i\omega t}$. The dependency in the y -plane is determined from the plate equations of motion.

The wavenumbers of plate j for the three different types of waves can be calculated from the equations below.

$$\text{Bending waves:} \quad k_B = \left(\frac{\rho_j \omega^2}{B_j} \right)^{1/4} \quad (4.1)$$

$$\text{Longitudinal waves:} \quad k_L^2 = \frac{\rho_j \omega^2 (1 - \vartheta_j^2)}{E_{y,j} h_j} \quad (4.2)$$

$$\text{Shear waves:} \quad k_S^2 = \frac{2\rho_j \omega^2 (1 + \vartheta_j)}{E_{y,j} h_j} \quad (4.3)$$

Where ρ_j is the mass per unit area, B_j is the bending stiffness, $E_{y,j}$ the Young's modulus, h_j the height of the plate and ϑ_j is Poisson's ratio. The response of the plate is assumed to have a y dependency of $e^{\mu y}$. This implies that μ must satisfy the equations 4.4-4.6, for the three types of waves.

$$\text{Bending waves:} \quad \mu_B^2 = k^2 \pm k_B^2 \quad (4.4)$$

$$\text{Longitudinal waves:} \quad \mu_L^2 = k^2 - k_L^2 \quad (4.5)$$

$$\text{Shear waves:} \quad \mu_S^2 = k^2 - k_S^2 \quad (4.6)$$

Here k is the adjacent leg of the incident wave type, further explained later in this chapter. Equation 4.4 has four roots, if $k > k_B$ two of the roots are real and positive and the other two are real and negative. Only the two negative roots

are significant in this case because the response must decay as $y \rightarrow \infty$. If $k < k_B$ the equation will yield two real roots and two negative. In this case the negative real root and the negative imaginary root is selected. For the longitudinal and shear wave types the equations will yield only one valid root for each wave type. The valid root is either real and negative or imaginary and negative.

The relationship between the edge displacement \mathbf{b}_j and the tractions \mathbf{F}_j can be written as equation 4.7.

$$\mathbf{F}_j = \mathbf{K}_j \mathbf{b}_j \quad (4.7)$$

Where \mathbf{K}_j can be seen as the dynamic stiffness matrix and the full matrix equation can be seen below.

$$\begin{bmatrix} T_j^F \\ N_j^F \\ S_j^F \\ M_j^F \end{bmatrix} = \begin{bmatrix} \alpha_{11} & \alpha_{12} & 0 & 0 \\ \alpha_{21} & \alpha_{22} & 0 & 0 \\ 0 & 0 & \alpha_{33} & \alpha_{34} \\ 0 & 0 & \alpha_{43} & \alpha_{44} \end{bmatrix} * \begin{bmatrix} u_{ej}^d \\ v_{ej}^d \\ w_{ej}^d \\ \theta_{ej}^d \end{bmatrix} \quad (4.8)$$

Where T_j^F , N_j^F , S_j^F and M_j^F are traction forces coordinates and u_{ej}^d , v_{ej}^d , w_{ej}^d and θ_{ej}^d are displacement coordinates, see Figure 4.2.

$$\alpha_{11} = -\frac{\mu_L(\mu_S^2 - k^2)}{2(1+\vartheta_j)} * \frac{E_{y,j}h_j}{k^2 - \mu_S\mu_L} \quad (4.9)$$

$$\alpha_{12} = -\frac{ik(\mu_S^2 + k^2 - 2\mu_L\mu_S)}{2(1+\vartheta_j)} * \frac{E_{y,j}h_j}{k^2 - \mu_S\mu_L} \quad (4.10)$$

$$\alpha_{21} = \left(\frac{ik(\mu_L^2 - \vartheta k^2)}{1 - \vartheta^2} - \frac{jk\mu_L\mu_S}{1 + \vartheta} \right) * \frac{E_{y,j}h_j}{k^2 - \mu_S\mu_L} \quad (4.11)$$

$$\alpha_{22} = \left(\frac{\mu_S(\vartheta k^2 - \mu_L^2)}{1 - \vartheta^2} + \frac{k^2\mu_S}{1 + \vartheta} \right) * \frac{E_{y,j}h_j}{k^2 - \mu_S\mu_L} \quad (4.12)$$

$$\alpha_{33} = (\mu_{B1}^2\mu_{B2} - \mu_{B2}^3\mu_{B1}) * \frac{B_j}{\mu_{B1} - \mu_{B2}} \quad (4.13)$$

$$\alpha_{34} = (\mu_{B2}^3 - \mu_{B1}^3 + (2 - \vartheta_j)(\mu_{B1} - \mu_{B2})k^2) * \frac{B_j}{\mu_{B1} - \mu_{B2}} \quad (4.14)$$

$$\alpha_{43} = (\mu_{B1}^2\mu_{B2} - \mu_{B2}^2\mu_{B1} + \vartheta_j k^2(\mu_{B1} - \mu_{B2})) * \frac{B_j}{\mu_{B1} - \mu_{B2}} \quad (4.15)$$

$$\alpha_{44} = (\mu_{B1}^2 - \mu_{B2}^2) * \frac{B_j}{\mu_{B1} - \mu_{B2}} \quad (4.16)$$

Equation 4.10, 4.11 and 4.15 were derived and modified compared to reference [9]. These erroneous equations were given in the article:

$$\alpha_{12} = -\frac{(\mu_S^2 - k^2)\mu_L}{2(1 + \vartheta_j)} * \frac{E_{y,j}h_j}{k^2 - \mu_S\mu_L} \quad (4.17)$$

$$\alpha_{21} = \left(\frac{ik(\mu_L^2 - \vartheta^2 k^2)}{1 - \vartheta^2} - \frac{jk\mu_L\mu_S}{1 + \vartheta} \right) * \frac{E_{y,j}h_j}{k^2 - \mu_S\mu_L} \quad (4.18)$$

$$\alpha_{43} = (\mu_{B2}^3 - \mu_{B1}^3 + (2 - \vartheta_j)(\mu_{B1} - \mu_{B2})k^2) * \frac{B_j}{\mu_{B1} - \mu_{B2}} \quad (4.19)$$

The compatibility conditions between the displacements \mathbf{a} of the plate carrying the incident wave and the edge displacements \mathbf{b}_j of the plate j are

$$\mathbf{b}_j = \mathbf{R}_j^T \mathbf{a} \quad (4.20)$$

where

$$\mathbf{a} = \begin{bmatrix} u^d \\ v^d \\ w^d \\ \theta^d \end{bmatrix} \quad (4.21)$$

$$\mathbf{b}_j = \begin{bmatrix} u_{ej}^d \\ v_{ej}^d \\ w_{ej}^d \\ \theta_{ej}^d \end{bmatrix} \quad (4.22)$$

$$\mathbf{R}_j = \begin{bmatrix} 1 & 0 & 0 & 0 \\ 0 & \cos \theta_j & -\sin \theta_j & 0 \\ 0 & \sin \theta_j & \cos \theta_j & 0 \\ 0 & 0 & 0 & 1 \end{bmatrix} \quad (4.23)$$

The angle θ_j is the plate-plate angle and is illustrated in Figure 4.1. To be able to solve equation 4.20 above one must first calculate the displacements in the junction; \mathbf{a} . This is done by calculating the complete equation which is a relation between the forces acting on the junction and plate displacement.

$$\left\{ \sum_{j=1}^N \mathbf{R}_j \mathbf{K}_j \mathbf{R}_j^T \right\} \mathbf{a} = \mathbf{R}_m \mathbf{f}_m \quad (4.24)$$

The notation m indicates the plate carrying the incident wave. \mathbf{f}_m can be calculated by using the equations 4.25-4.26.

In the case of the incident wave being carried in the plate j equation 4.7 is not valid. Then \mathbf{F}_j must be replaced by $\mathbf{F}_j - \mathbf{F}'_j$ and \mathbf{b}_j by $\mathbf{b}_j - \mathbf{b}'_j$. \mathbf{F}'_j and \mathbf{b}'_j are the edge displacement and tractions caused by the incident wave. With this in mind equation 4.7 then becomes

$$\mathbf{F}_j = \mathbf{K}_j \mathbf{b}_j - \mathbf{f}_j \quad (4.25)$$

$$\mathbf{f}_j = \mathbf{K}_j \mathbf{b}'_j - \mathbf{F}'_j \quad (4.26)$$

Where \mathbf{f}_j can be seen as a dynamic loading vector acting on the semi-infinite plate.

Depending on the type of wave that is incident on the junction the components of \mathbf{F}'_j and \mathbf{b}'_j differs.

In case of an incident bending wave with an angle ϕ is approaching the connecting edge the components of \mathbf{F}'_j and \mathbf{b}'_j are.

$$\mathbf{F}'_j = \begin{bmatrix} T_j^{F'} \\ N_j^{F'} \\ S_j^{F'} \\ M_j^{F'} \end{bmatrix} = \begin{bmatrix} 0 \\ 0 \\ -\alpha B_j (\mu^3 - (2 - \nu_j) k^2 \mu) \\ \alpha B_j (\mu^2 - \nu_j k^2) \end{bmatrix} \quad (4.27)$$

$$\mathbf{b}'_j = \begin{bmatrix} u_{ej}^{d'} \\ v_{ej}^{d'} \\ w_{ej}^{d'} \\ \theta_{ej}^{d'} \end{bmatrix} = \begin{bmatrix} 0 \\ 0 \\ \alpha \\ \alpha \mu \end{bmatrix} \quad (4.28)$$

Where α is the wave amplitude and

$$k = k_B * \cos(\phi) \quad (4.29)$$

$$\mu = i k_B * \sin(\phi) \quad (4.30)$$

If a longitudinal wave is incident the components are

$$\mathbf{F}'_j = \begin{bmatrix} T_j^{F'} \\ N_j^{F'} \\ S_j^{F'} \\ M_j^{F'} \end{bmatrix} = \begin{bmatrix} \alpha E_{y,j} h_j k \mu / (1 + \vartheta_j) \\ i \alpha E_{y,j} h_j (\mu^2 - \vartheta_j k^2) / (1 - \vartheta_j^2) \\ 0 \\ 0 \end{bmatrix} \quad (4.31)$$

$$\mathbf{b}'_j = \begin{bmatrix} u_{ej}^{d'} \\ v_{ej}^{d'} \\ w_{ej}^{d'} \\ \theta_{ej}^{d'} \end{bmatrix} = \begin{bmatrix} \alpha k \\ i \alpha \mu \\ 0 \\ 0 \end{bmatrix} \quad (4.32)$$

where

$$k = k_L * \cos(\phi) \quad (4.33)$$

$$\mu = i k_L * \sin(\phi) \quad (4.34)$$

The last case is the incident shear wave

$$\mathbf{F}'_j = \begin{bmatrix} T_j^{F'} \\ N_j^{F'} \\ S_j^{F'} \\ M_j^{F'} \end{bmatrix} = \begin{bmatrix} i \alpha E_{y,j} h_j (\mu^2 + k^2) / 2(1 + \vartheta_j) \\ -\alpha E_{y,j} h_j k \mu / (1 + \vartheta_j) \\ 0 \\ 0 \end{bmatrix} \quad (4.35)$$

$$\mathbf{b}'_j = \begin{bmatrix} u_{ej}^{d'} \\ v_{ej}^{d'} \\ w_{ej}^{d'} \\ \theta_{ej}^{d'} \end{bmatrix} = \begin{bmatrix} i \alpha \mu \\ -\alpha k \\ 0 \\ 0 \end{bmatrix} \quad (4.36)$$

where

$$k = k_S * \cos(\phi) \quad (4.37)$$

$$\mu = i k_S * \sin(\phi) \quad (4.38)$$

By using equation 4.24 \mathbf{a} is calculated and the response displacement \mathbf{b}_j by plate j can be obtained with equation 4.20. The corresponding amplitudes in plate j can now be calculated by the use of equation 4.39 below.

$$\begin{bmatrix} u_{ej}^d \\ v_{ej}^d \\ w_{ej}^d \\ \theta_{ej}^d \end{bmatrix} = \begin{bmatrix} k & i\mu_S & 0 & 0 \\ i\mu_L & -k & 0 & 0 \\ 0 & 0 & 1 & 1 \\ 0 & 0 & \mu_{B1} & \mu_{B2} \end{bmatrix} * \begin{bmatrix} \alpha_L \\ \alpha_S \\ \alpha_{B1} \\ \alpha_{B2} \end{bmatrix} \quad (4.39)$$

The corresponding power of the wave amplitude for the different types of waves can be calculated as follows:

$$P_B = (\rho_j \omega^3 \alpha^2 / k_B) \sin \phi \quad (4.40)$$

$$P_L = \frac{\rho_j \omega^3 \alpha^2 k_L \sin \phi}{2} \quad (4.41)$$

$$P_S = \frac{\rho_j \omega^3 \alpha^2 k_S \sin \phi}{2} \quad (4.42)$$

With equations 4.40-4.42 above the transmitted power can be calculated by using the appropriate amplitude and transmitted wave heading, see equation 4.43.

$$\phi_r = \cos^{-1} \frac{k}{k_r} \quad (4.43)$$

Where k_r is the wavenumber of the transmitted wave type and k is the wavenumber of the incident.

Finally the transmission coefficient may be calculated by taking the ratio of the transmitted power to the total power which is incident on the junction.

The transmission coefficients can be written in a general form $\tau_{pr}^{ij}(\omega, \phi)$ where i, p, ω and ϕ represents the carrying plate, wave type, frequency and heading. The plate and wave type of the generated wave is represented by j and r . In case of $i=j$ the coefficient is referred to as reflection coefficient rather than transmission coefficient. Since no energy is assumed to be dissipating in the junction the conservation of energy must be fulfilled, see equation 4.44.

$$\sum_r \sum_j \tau_{pr}^{ij}(\omega, \phi) = 1 \quad (4.44)$$

Finally the diffuse field transmission coefficient, which is the parameter used in the program, can be calculated by the integral below.

$$\tau_{pr}^{ij}(\omega) = \frac{1}{2} \int_0^{\pi} \tau_{pr}^{ij}(\omega, \phi) \sin(\phi) d\phi \quad (4.45)$$

The number of angles determines the accuracy of the transmission coefficient. Stated in reference [10] integration over 100 angles will generate a difference in result with up to 0.1 - 1 dB and a corresponding value of 10.000 angles will generally provide a result better than 0.01dB. The default number of angles is 1000 in SEALab but can easily be changed by the user.

4.2 Radiation efficiency from finite plates

The interaction between a plate and its surrounding medium is of great interest. The medium surrounding the plate can be of any type of medium, such as air, water or any other type of fluid or gas. The interaction is described by the radiation factor for free waves and can be calculated with several different methods. The approach explained here are according to standard EN12354-1 [4] and shown in equations 4.46-4.62.

There are two important frequencies to consider when calculating the radiation factors. The first one is the frequency for the first mode in both x- and y-direction of the plate, f_{11} . Which is calculated according to equation 4.46 below:

$$f_{11} = \frac{c_0^2}{4f_c} \left(\frac{1}{l_1^2} + \frac{1}{l_2^2} \right) \quad (4.46)$$

Where c_0 is the speed of which the wave propagates in the surrounding medium, l_1 and l_2 are the dimensions of the plate and f_c is the second important frequency, the critical frequency of the plate. This is given by 4.47 below:

$$f_c = \frac{c_0^2}{1.8c_L t} \quad (4.47)$$

Where c_L is speed of which a longitudinal wave propagates in the plate and t is the plate thickness in meters.

Depending on the two frequencies f_{11} and f_c the radiation efficiency is calculated in different ways:

If $f_{11} \leq f_c/2$ then:

$$\sigma = \sigma_1 \quad f \geq f_c \quad (4.48)$$

$$\sigma = \frac{2(l_1+l_2)c_0}{l_1l_2 f_c} \delta_1 + \delta_2 \quad f < f_c \quad (4.49)$$

$$\text{Where} \quad \delta_1 = \frac{(1-\lambda^2) \ln \frac{1+\lambda}{1-\lambda} + 2\lambda}{4\pi^2(1-\lambda^2)^{1.5}} \quad (4.50)$$

$$\text{with } \lambda = \sqrt{\frac{f}{f_c}} \quad (4.51)$$

$$\text{and} \quad \delta_2 = 0 \quad f > f_c/2 \quad (4.52)$$

$$\delta_2 = \frac{8c_0^2(1-2\lambda^2)}{f_c^2 \pi^4 l_1 l_2 \lambda \sqrt{1-\lambda^2}} \quad f \leq f_c/2 \quad (4.53)$$

$$\sigma = \sigma_2 \quad \left\{ \begin{array}{l} f < f_{11} < f_c/2 \\ \text{and} \\ \sigma > \sigma_2 \end{array} \right. \quad (4.54)$$

$$\sigma \leq 2.0 \quad (4.55)$$

If $f_{11} > f_c/2$ then:

$$\sigma = \sigma_2 \quad f < f_c \text{ and } \sigma_2 < \sigma_3 \quad (4.56)$$

$$\sigma = \sigma_1 \quad f > f_c \text{ and } \sigma_1 < \sigma_3 \quad (4.57)$$

$$\text{else: } \sigma = \sigma_3 \quad (4.58)$$

$$\sigma \leq 2.0 \quad (4.59)$$

Where the radiation factor parts σ_{1-3} is calculated according to equations 4.59-4.61.

$$\sigma_1 = \frac{1}{\sqrt{1-f_c/f}} \quad (4.60)$$

$$\sigma_2 = 4l_1l_2 \left(\frac{f}{c_0}\right)^2 \quad (4.61)$$

$$\sigma_3 = \sqrt{\frac{2\pi f(l_1+l_2)}{16c_0}} \quad (4.62)$$

4.3 Non-resonant transmission

SEA is mainly a technique for calculating responses for resonant transmission between subsystems. Although for coupling between rooms separated by a single or doubled leaf wall there is transmission through the separating wall below the resonance frequency of the leafs. This type of transmission is called non-resonant transmission and is modeled as a path between the two rooms neglecting the wall. The wall is included in the model once it becomes resonant. Examples of this can be found in chapter 5 that concerns the validation of the software. The approximations used to calculate non-resonant transmission is often simplified to be computationally possible and can be calculated by the following formulas [4]:

$$\tau = \left(\frac{2\rho_0c_0}{2\pi f\rho}\right)^2 \frac{\pi f_c \sigma^2}{2f\eta_{tot}} \quad (4.63)$$

Where f_c , σ , ρ and η_{tot} are the critical frequency, radiation efficiency, density per unit area and total losses of the plate. ρ_0 and c_0 are the density and speed of sound properties of the sending room. Equation 4.63 is used to calculate the non-resonant transmission trough a single leaf wall and is of course only valid below the critical frequency.

In the case of non-resonant transmission through a double leaf wall there are a set of simplified equations which are based on an empirical model and were the cavity is assumed to be filled with a porous absorber [8]:

$$R \begin{cases} R_M & f < f_{dw} & (4.64) \\ R_1 + R_2 + 20\log_{10}(fd) - 29 & f_{dw} < f < f_d & (4.65) \\ R_1 + R_2 + 6 & f > f_d & (4.66) \end{cases}$$

R is called sound reduction index and it is a value of the sound insulation provided by the wall. When using these formulas R is simply defined as

$$R = 20 \log_{10}(fm) - 47 \quad (4.67)$$

R_1 and R_2 are the reduction of leaf 1 and 2. Below the double leaf wall resonance frequency f_{dw} the two leafs can be modeled as rigidly connected and then R_M is calculated by adding the masses of the two leaf and using equation 4.66. The double leaf wall resonance frequency is calculated by equation 4.68 below.

$$f_{dw} = \frac{1}{2\pi} \sqrt{\frac{K(m_1+m_2)}{m_1 m_2}} \quad (4.68)$$

Where K can be seen as the spring-stiffness created by the air between the two separated panels.

$$K = \frac{\rho c^2}{d} \quad (4.69)$$

Here d is the width of the cavity separating the two leafs. There is a certain frequency when the cavity stops acting like a spring with constant stiffness. This frequency is given by

$$f_d = \frac{55}{d} \quad (4.70)$$

The transmission factor, which is needed for the CLF-calculation, can easily be calculated by the formula:

$$\tau = 10^{-R/10} \quad (4.71)$$

5 Validation

This chapter concerns the validation of the calculations made in SEALab. The results have been compared to reference [9] and a commercial software called AutoSEA v.1.5.

Three typical cases were chosen as reference; plate-plate transmission, single and double leaf wall transmission. The calculations of the plate-plate transmission were validated to reference [9] and AutoSEA. The two cases of airborne sound transmission were compared to AutoSEA.

When analyzing plate-plate transmission the results from SEALab are first compared to reference [9] and presented as transmission coefficients as a function of incident angle and diffuse field transmission coefficients as a function of plate angle. The quantities used to compare the results to AutoSEA are the transmitted energies and modal energies of the three wave types. The influence on the transmitted energy levels by the number of incident angles used is also presented.

In the case of airborne sound transmission the results are compared to AutoSEA and is presented as input power, total energy and modal energy for the last subsystem in the system; the adjacent room.

The results are quantitatively described in this chapter, qualitative discussion is presented in chapter 6.

5.1 Structural transmission coefficients

The transmission coefficients have been calculated according to ref [9] as described in the previous chapter.

First the transmission coefficient as a function of incident angle will be presented and compared for a case where two isotropic plates are coupled over an angle of 90° . Both plates are identical and are chosen so that the Poisson's number is set to 0.3 and the frequency is chosen so that the ratio between the longitudinal wavenumber k_L and the bending wavenumber k_B is given by $k_L/k_B=0.3$.

The calculations were done over one thousand incident angles evenly spread out over the junction. The transmission and reflection coefficients and the sum of these for an incident bending wave are presented in figure 5.1 below. Each line represents one of three transmitted wave types.

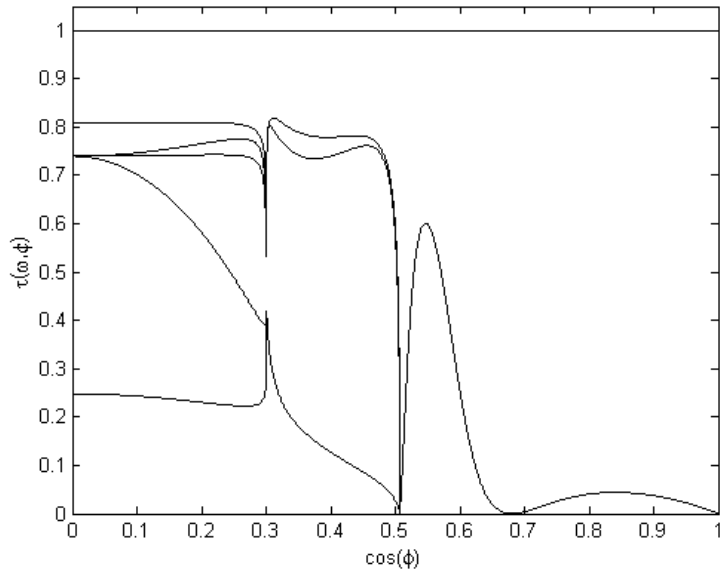


Figure 5.1 Transmission coefficient as a function of incident angle calculated in SEALab

The same results have also been presented by reference [9] and can be seen in Figure 5.2 below.

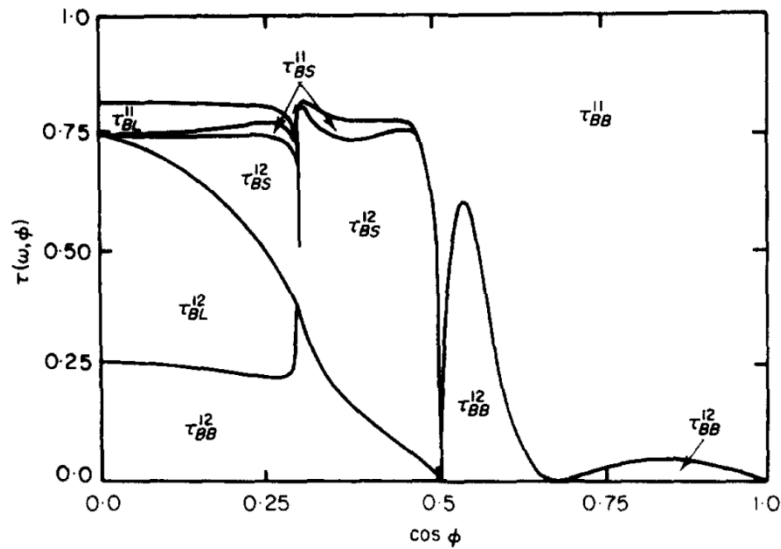


Figure 5.2 Transmission coefficient as a function of incident angle. Reprint from ref [9] with permission from Elsevier

The incident angle representing $\cos(\phi) = 0.3$ is the critical angle for transmitted longitudinal waves; above this angle no longitudinal waves are transmitted. The corresponding angle for shear waves is $\cos(\phi) = 0.507$.

For comparisons of Figure 5.1 and Figure 5.2 it shows that the result corresponds well with each other over all incident angles. The summations of the transmission and reflection coefficients are equal to 1, which verifies that no energy is lost or gained in the junction in accordance to equation 4.44.

As a second test the transmission coefficients were calculated for two identical plates with the same characteristics as the case above and for the same frequency. This time the diffuse transmission coefficient is plotted as a function of coupling angle. The diffuse field transmission coefficients for bending, longitudinal and shear waves were calculated with the same resolution of the incident waves as before (one thousand incident angles). The calculated transmission coefficients as a function of coupling angle are presented in Figure 5.3. The same case has been presented by reference [9] and can be seen in Figure 5.4.

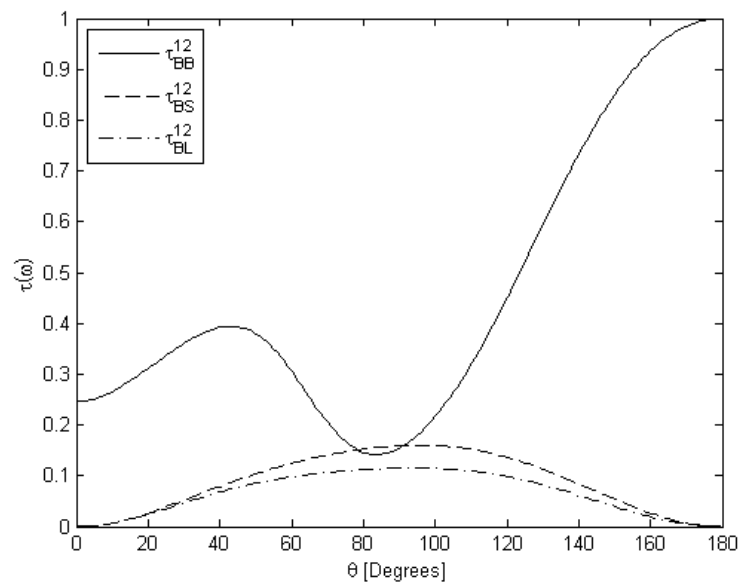


Figure 5.3 Diffuse transmission coefficients as a function of plate angle calculate by SEAlab

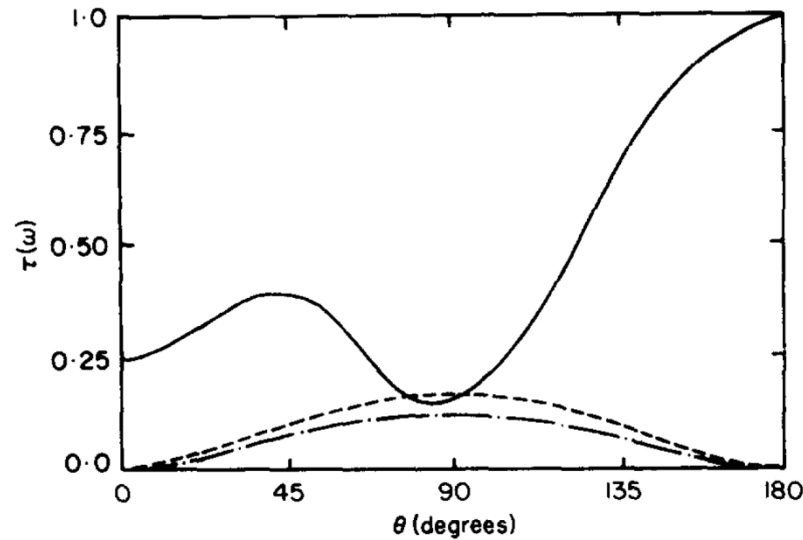


Figure 5.4 Diffuse transmission coefficients as a function of plate angle. Reprint from ref [9] with permission from Elsevier

From comparisons of Figure 5.3 and Figure 5.4 it shows that they match each other very well for the three wave types and all degrees of the plate angles; 0-180 degrees.

As a second part of the plate-plate transmission validation a plate-plate transmission is considered and calculated. The results are compared to AutoSEA. In this case two steel plates are connected in a line junction and the setup is:

Two steel plates connected in a line junction with an angle of 120°. The length of the junction is 1m.

The plates are identical and have the following properties:

$$E = 207 \text{ GPa}$$

$$\rho = 7820 \text{ kg/m}^3$$

$$\vartheta = 0.29$$

Plate dimensions: 1 m * 1 m * 0,001 m

Plate 1 is excited with bending waves which has an input power for every one-third octave band of approximately 1.26W. The results are plotted as the wave type energy in plate 2 and are presented in two figures; compared to and relative to AutoSEA. The diffuse transmission coefficients were calculated with 1000 incident angles.

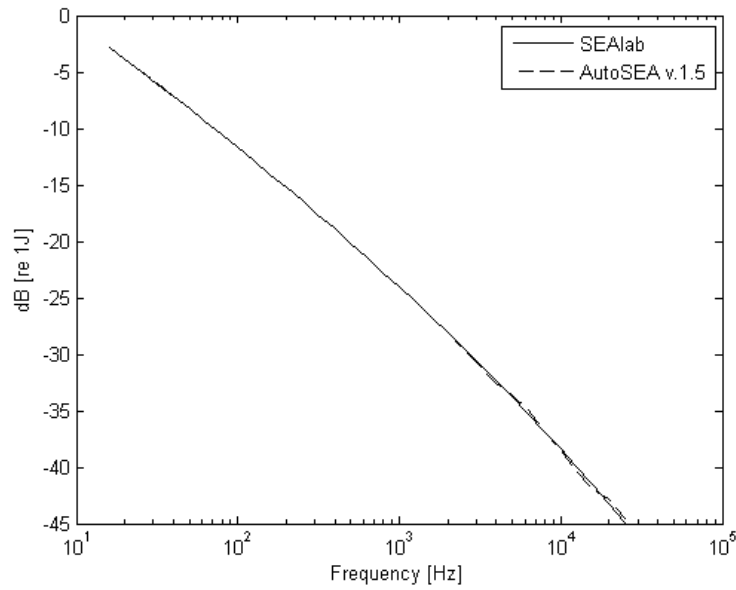


Figure 5.5 SEALab and AutoSEA comparison of the transmitted bending wave energy

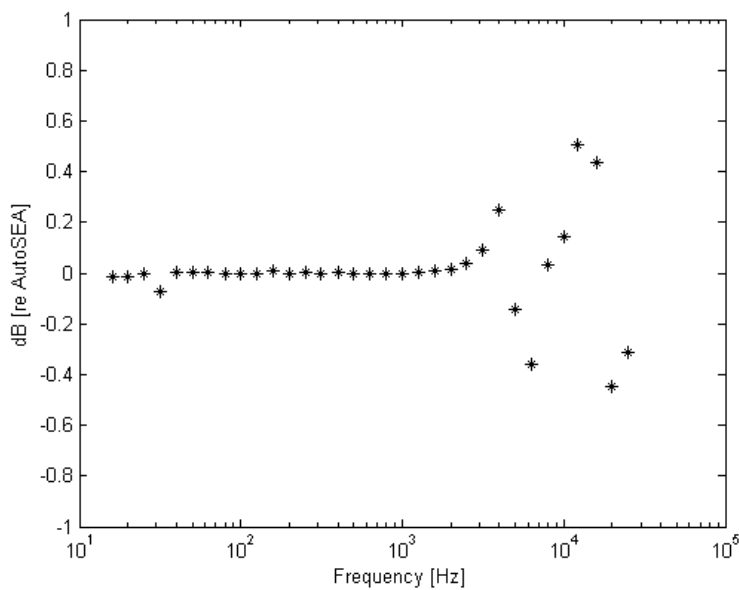


Figure 5.6 Transmitted bending wave energy for SEALab in dB relative AutoSEA

Figure 5.5 and Figure 5.6 clearly shows a good correlation between the two results over a wide frequency range. There are some deviations above 4000Hz. The largest deviation occurs at 12220 Hz and is 0.5dB.

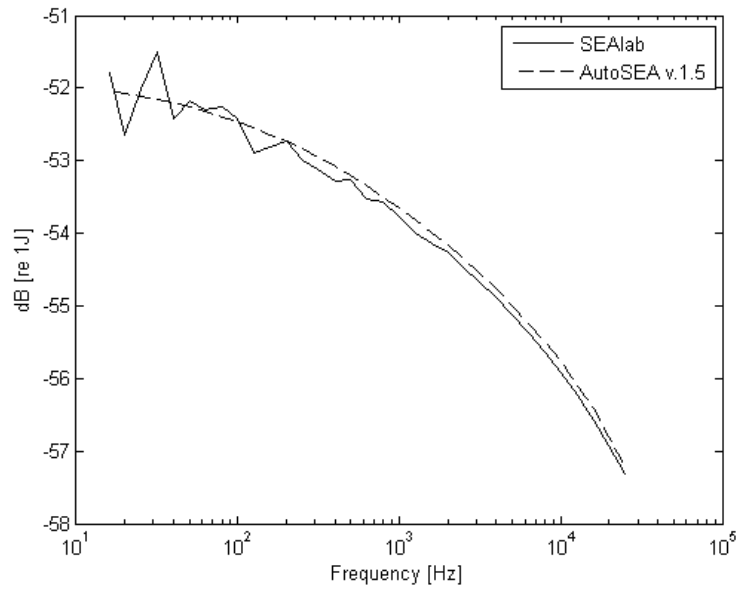


Figure 5.7 SEALab and AutoSEA comparison of the transmitted longitudinal wave energy

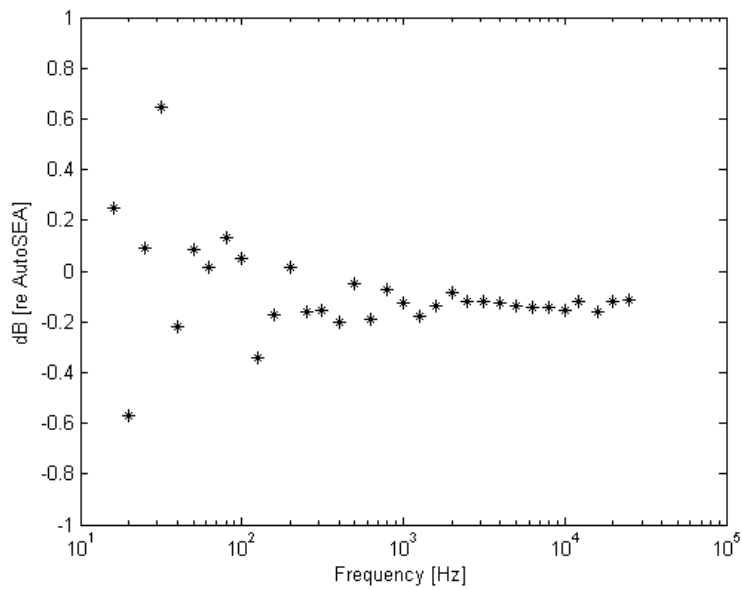


Figure 5.8 Transmitted longitudinal wave energy for SEALab in dB relative AutoSEA

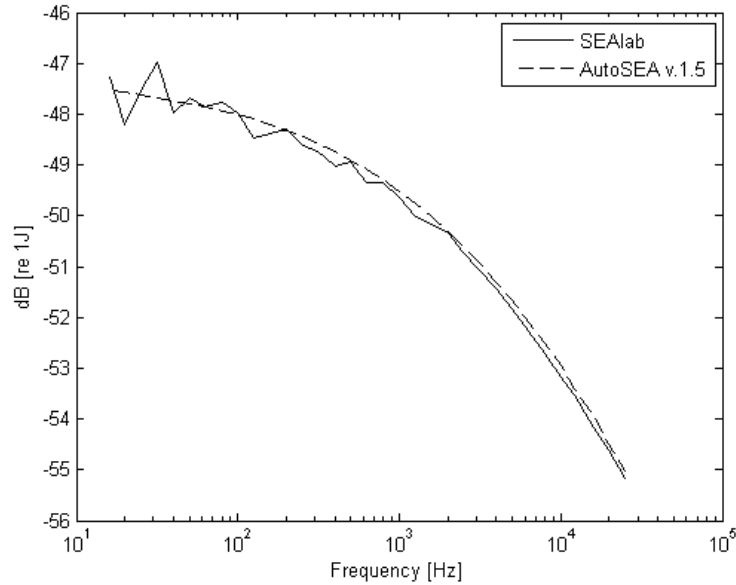


Figure 5.9 SEALab and AutoSEA comparison of the transmitted shear wave energy

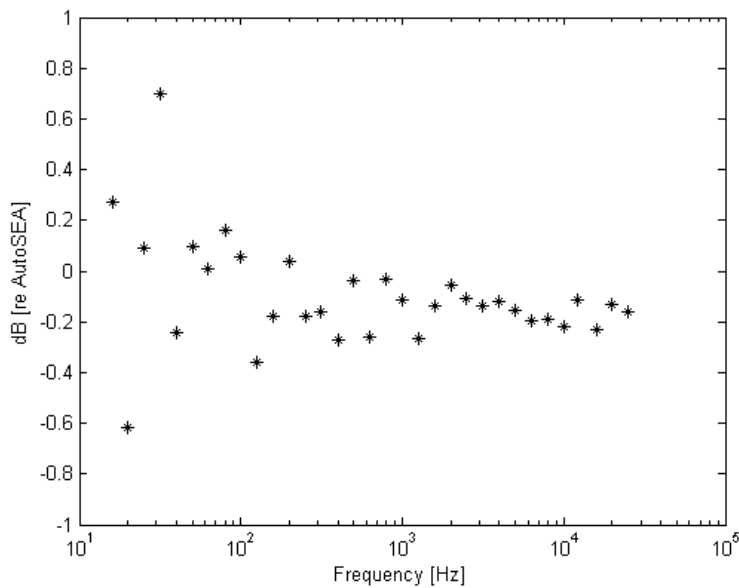


Figure 5.10 Transmitted shear wave energy for SEALab in dB relative AutoSEA

The two generated wave types, longitudinal and shear waves, shows similar behavior, Figure 5.7 - Figure 5.10. The deviation is larger for lower frequencies but becomes better for higher frequencies. The largest deviation for longitudinal and shear waves occurs at 32 Hz with a deviation of 0.65 dB for longitudinal waves and 0.7dB for shear waves.

The number of incident angles used in SEALab is important for the result. In the following the calculated energy in the second plate is presented as calculations of 1000 incident angles compared to 100 and 10000 incident angles.

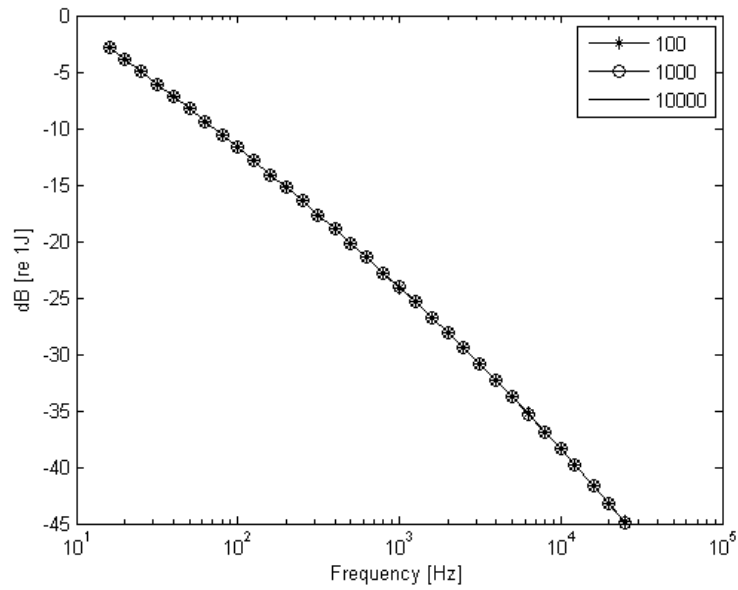


Figure 5.11 Transmitted bending wave energy comparison depending on the number of incident angles used

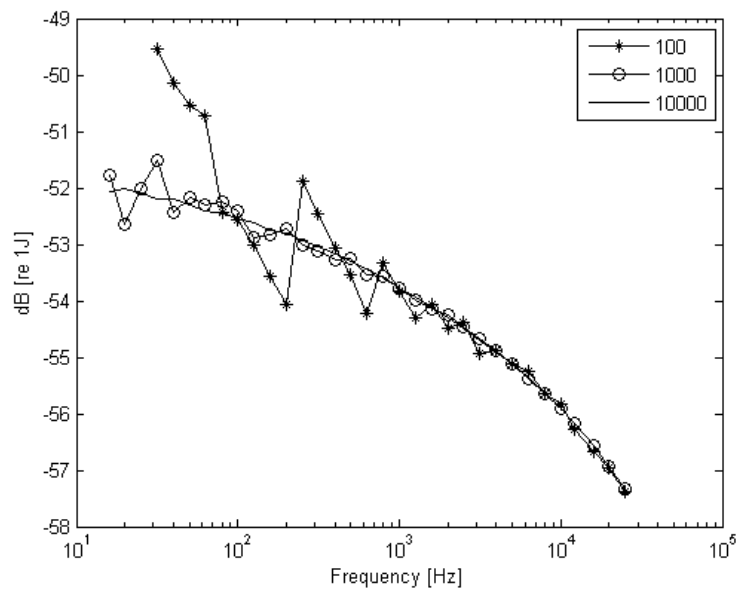


Figure 5.12 Transmitted longitudinal wave energy comparison depending on the number of incident angles used

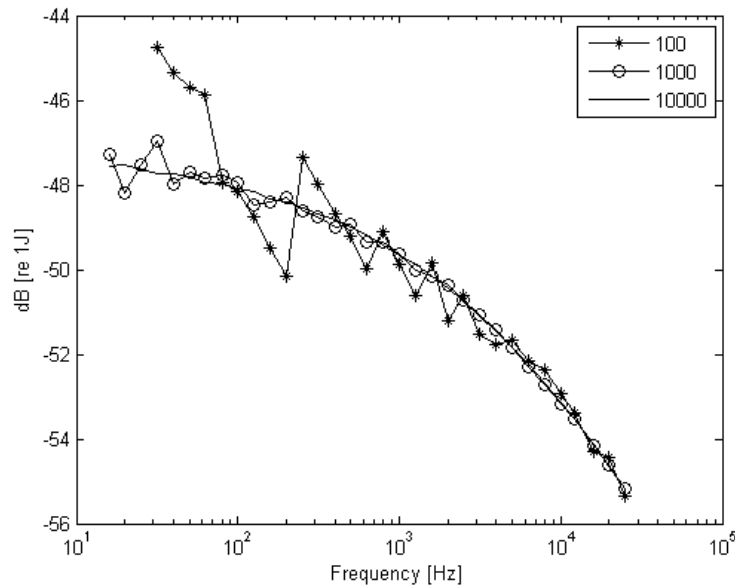


Figure 5.13 Transmitted shear wave energy comparison depending on the number of incident angles used

The influence of the number of angles used has little effect on the bending wave type. For longitudinal and shear wave type the difference in result is mainly located at low frequencies, which is where the largest deviations were located according to Figure 5.7 - Figure 5.10.

As described in chapter 2.9 there are several restrictions when modeling in SEA that must be fulfilled in order to obtain relevant results. The equations used for calculating the upper frequency limits, equation 3.53 and 3.54, are satisfied in the calculated frequency interval except for bending waves which does not fulfill unity of equation 3.53 for frequencies above 10000Hz.

According to the modal overlap the lower frequency limit for the three wave types are; 315Hz for bending waves, 16000Hz for shear waves and 25000Hz for longitudinal waves. Combining the limits results in the following valid ranges:

Bending waves: 315-10000Hz

Longitudinal waves: 16000Hz - >

Shear waves: 25000Hz - >

5.2 Single leaf wall

The sound transmission through a single leaf wall between two rooms for a specific case will be presented and compared to the results for an identical case calculated with AutoSEA.

The schematics of a single leaf wall construction can be seen in Figure 5.14.

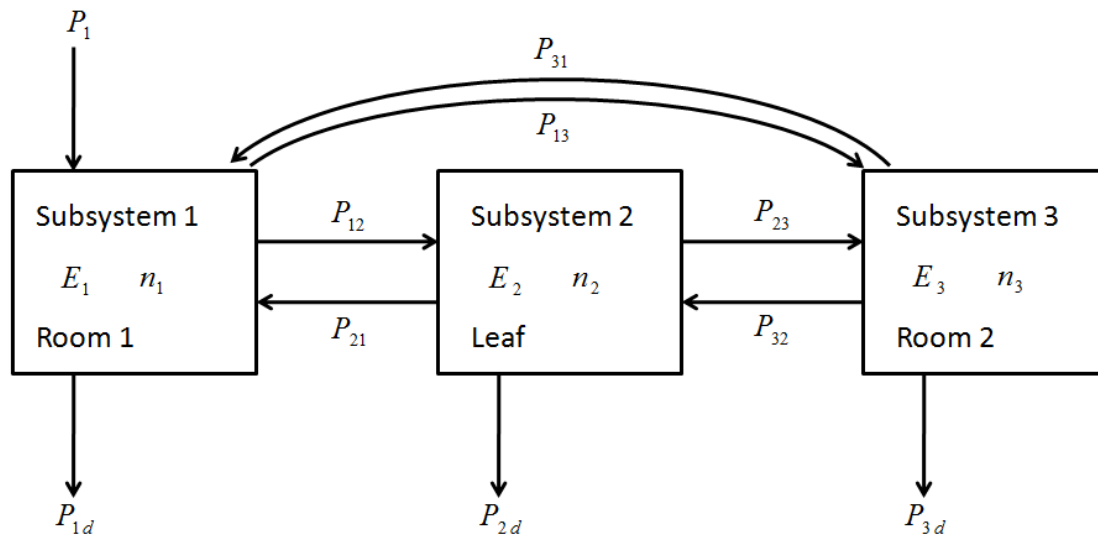


Figure 5.14 Schematics of the subsystems and the power flows for a single-leaf wall

The system in consideration consists of two identical rooms (subsystem 1 & 3) which have the properties:

Fluid: *Air*

Volume, $V = 3 * 3 * 3 = 27m^3$

Surface, $S' = 6(3 * 3) = 53m^2$

Perimeter length, $L' = 12 * 3 = 36m$

The properties of the plate separating the two rooms (subsystem 2) are:

Material: *Gypsum*

Dimensions: $3 * 3 * 0.01m$

$E = 4.1 \text{ GPa}$

$\vartheta = 0.3$

$\rho = 850 \times 0.01 \text{ kg/m}^2$

$f_c \approx 2800\text{Hz}$

The total loss factor η_2 for the plate was calculated according to the calculation method for structural coupling described in chapter 3. Three plates were coupled as a T-junction where the “roof” of the T was 5 cm thick concrete plates and the perpendicular plate was the gypsum plate separating the two rooms described above. The losses for this model were multiplied by four representing losses to the floor, ceiling and the two side walls. The losses from the plate to its surrounding air were also accounted for as well as the internal losses. Including a loss factor $\eta_{2,d}$ of 0.01 all of the losses accumulate to a total loss factor η_2 of roughly 0.02.

The calculations were made in one-third octave bands with a range of 16-25000Hz. The input power for every one-third octave band was approximately 1.26W.

The results from the calculations can be seen in Figure 5.15-Figure 5.19 below.

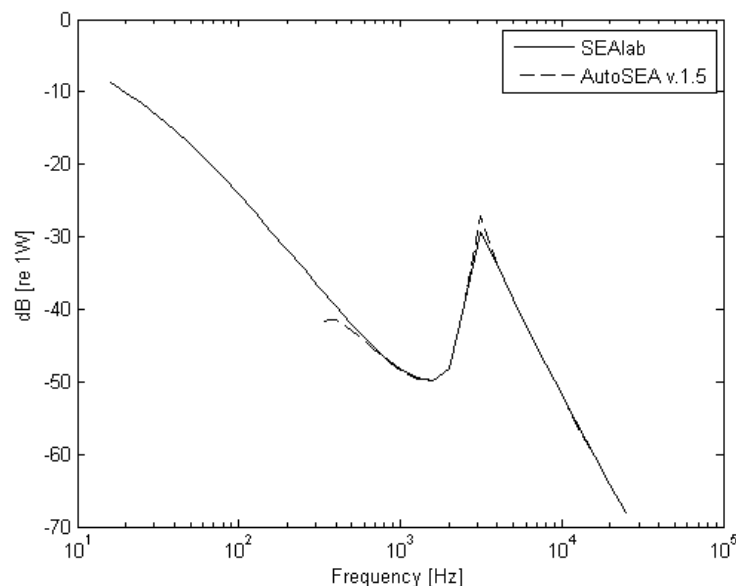


Figure 5.15 Resonant power input from subsystem 2 to subsystem 3 compared to AutoSEA

Figure 5.15 shows transmitted power from the gypsum wall to the second room, P_{12} (resonant transmission). The results show a well correlation between the two software. AutoSEA does not calculate below 315 Hz. In the frequency range of 315- 25000Hz the correlation is good. There are some deviations at 315 Hz and at the resonance peak; 3150 Hz.

The non resonant sound transmission between the two rooms presented as the power transmitted from subsystem 1 to subsystem 3, P_{13} is presented in Figure 5.16.

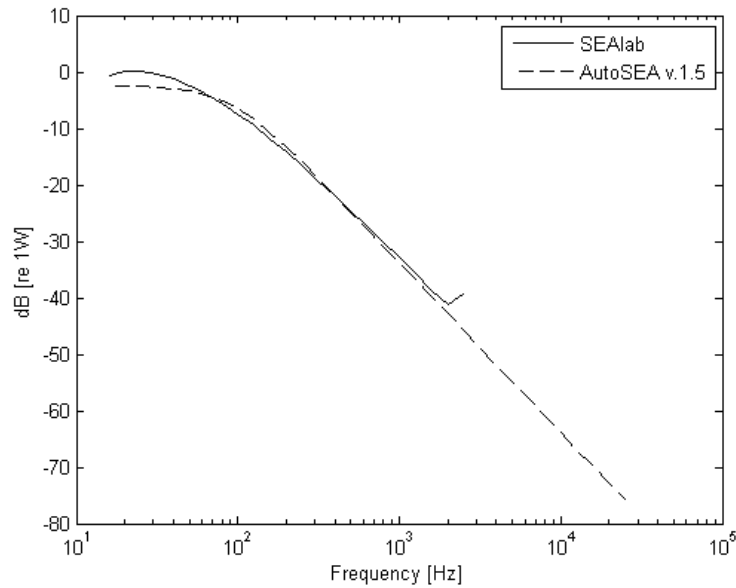


Figure 5.16 Non-resonant input power from subsystem 1 to subsystem 3 compared to AutoSEA

As can be seen in Figure 5.16 SEAlab does not calculate any non-resonant transmission for frequencies at or above the resonance frequency of the separating leaf. Therefore there are no results from SEAlab for frequencies above 2500 Hz. The two plots match well in the frequency range 63 – 2000 Hz.

The total energy in subsystem 3 can be seen in Figure 5.17. The difference between the calculations and the results from AutoSEA can then be seen in Figure 5.18 which shows the calculated energy in dB relative the results from AutoSEA.

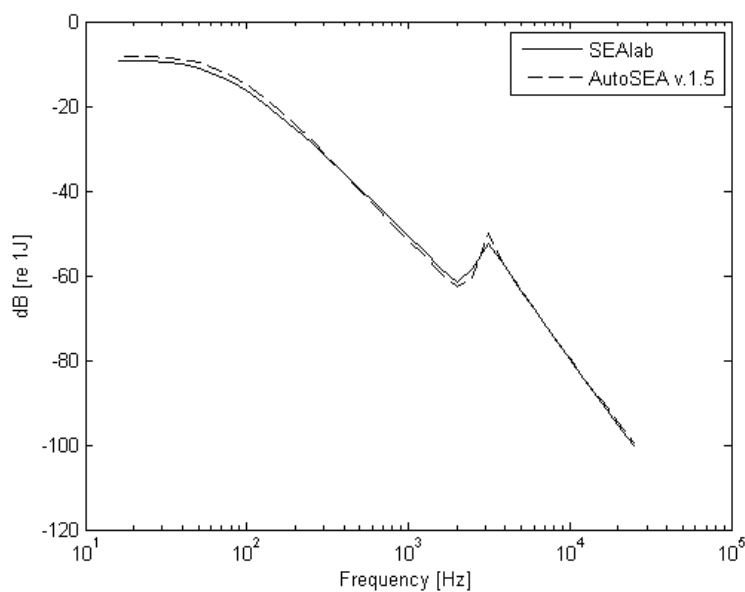


Figure 5.17 Energy subsystem 3 compared to AutoSEA

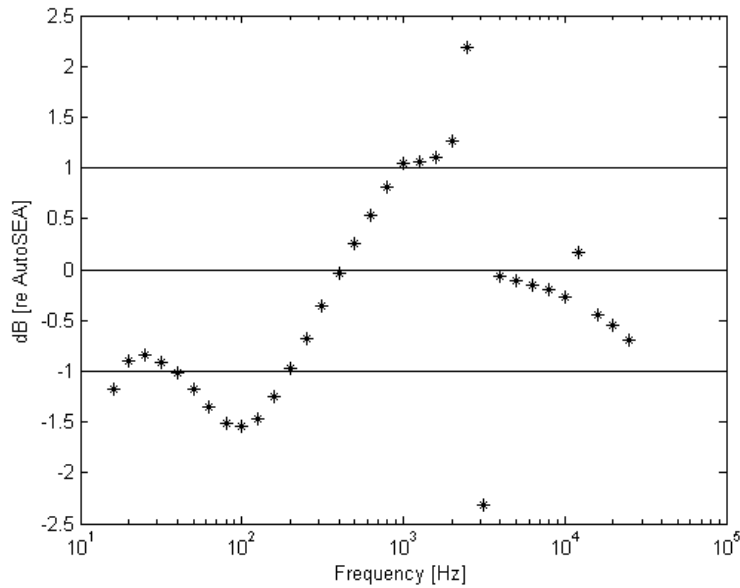


Figure 5.18 Energy of subsystem 3 described as the SEALab result relative AutoSEA results

Figure 5.17 and Figure 5.18 shows the total energy in subsystem 3; room 2. There are some deviations compared to AutoSEA. The largest deviation occurs around the resonance frequency and is at worst almost 2.5 dB. Excluding the frequencies around the resonance frequency the deviation is around 1 dB for frequencies below the resonance frequency. Above the resonance frequency the result becomes better with the largest deviation of 0.7dB at 2500 Hz.

Instead of total energy, the modal energy is presented in Figure 5.19 and shows the same tendencies as the calculated energy.

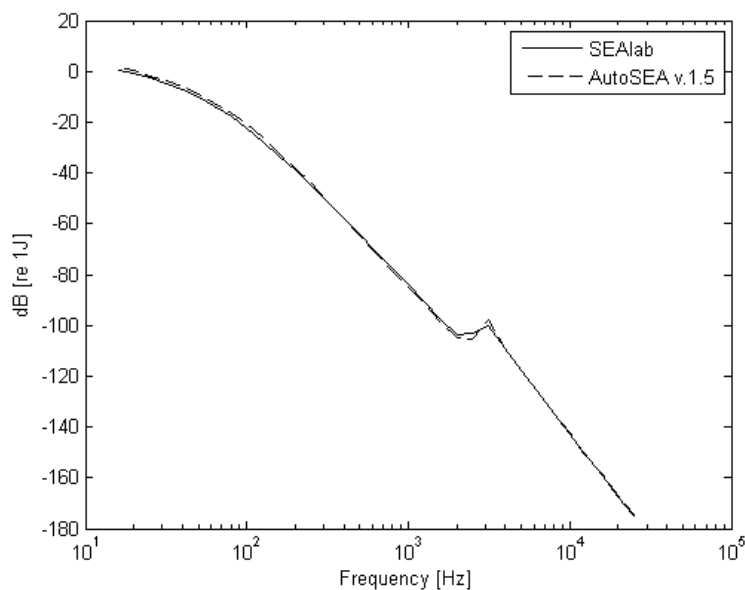


Figure 5.19 Modal energy in subsystem 3 compared to AutoSEA

In order to obtain accurate results the assumptions made in SEA needs to be fulfilled. In order for the assumption made that the Euler-Bernoulli plate theory is valid, the relation between the wavelength and thickness of the plate must satisfy the expression stated in equation 3.54. When calculated for bending waves the frequency limit is higher than the frequency spectra used.

Another assumption that sets a frequency limit of the SEA model is that the energy a wave traveling across the plate carries is not damped too much, this is described in equation 3.53. The length of the plate is 3m and will give a upper frequency limit of 5.000 Hz for bending waves, 12.200 Hz for longitudinal waves and 8.000 Hz for shear waves.

A third assumption that sets a frequency limit of the SEA model is the modal overlap requirement. This is explained in equation 3.46 which states that the modal overlap should be greater than unity, otherwise the subsystem is not damping controlled. The modal overlap becomes greater than one for bending waves when the frequency is higher than 160Hz, 3.150Hz for longitudinal and 2.000Hz for shear waves. These limits will set a total frequency span where the SEA model is assumed to give the most accurate results. When summed up the frequency spans looks like:

Bending waves: 160 – 5.000 Hz

Longitudinal waves: 3.150 – 12.220 Hz

Shear waves: 2.000 – 8.000 Hz

For all wave types in the leaf the three assumptions discussed will be fulfilled in the frequency range: 3.150 – 5.000 Hz.

Taking 3m as the maximum length of the room the requirement of relatively constant energy (equation 3.53) is satisfied for one-third octave bands below 1.600 Hz. Modal overlap (equation 3.46) is fulfilled for one-third octave bands above 200 Hz for the two rooms which give a valid frequency span of 200 Hz – 1.600 Hz.

5.3 Double leaf wall example

The sound transmission through a double leaf wall for a specific case will be presented and compared with results from an identical case calculated in AutoSEA. The system is modeled in the same way as reference [3] and reference [8] to calculate the energies for a double wall. The setup for this system can be seen in Figure 5.20.

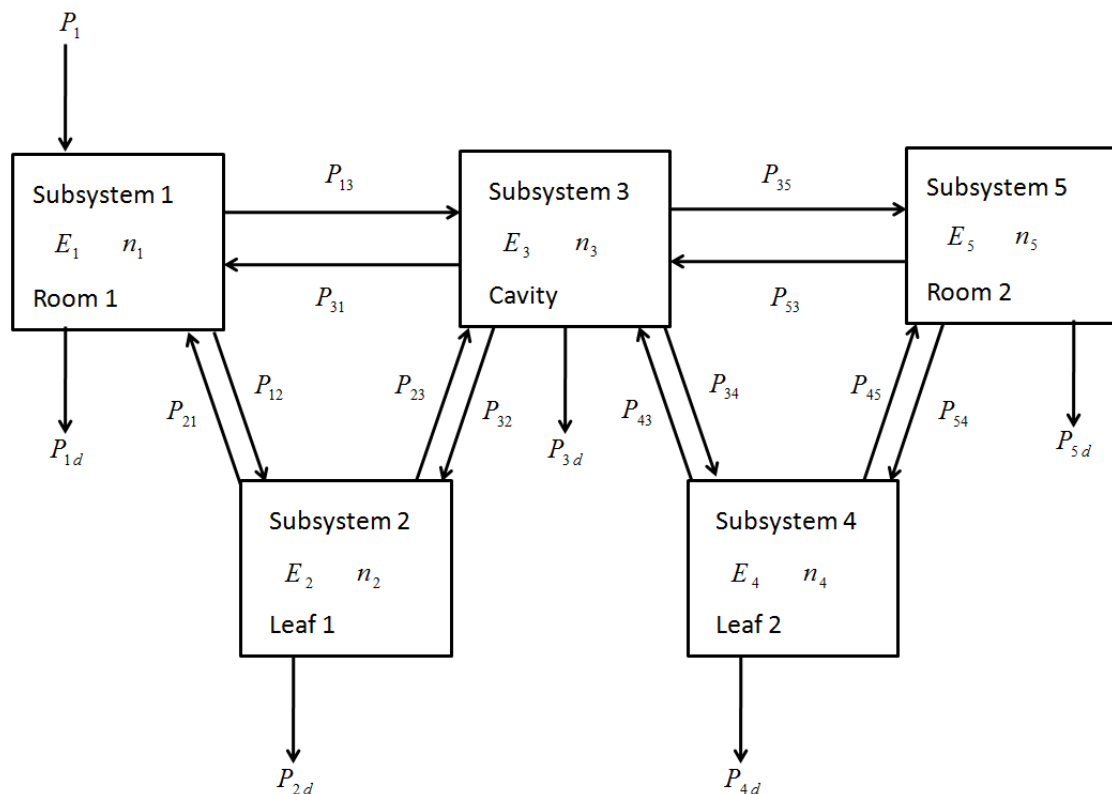


Figure 5.20 Schematics of the subsystems and the power flows for a double-leaf wall

The system consists of five subsystems, these are the two rooms (subsystem 1 and 5), the cavity inside the wall (subsystem 3) and the two leaves of the wall (subsystems 2 and 4).

The two rooms (subsystems 1 and 5) are identical and have the properties:

Fluid: *Air*

Volume, $V = 3 * 3 * 3 = 27m^3$

Surface, $S' = 6(3 * 3) = 53m^2$

Perimeter length, $L' = 12 * 3 = 36m$

The cavity (Subsystem 3) is modeled as:

Fluid: *Air*

$$\text{Volume, } V = 3 * 3 * 0.1 = 0.9m^3$$

$$\text{Surface, } S' = 2(3 * 3 + 3 * .1 + 3 * .1) = 19.2m^2$$

$$\text{Perimeter length, } L' = 4(3 + 3 + .1) = 24.4m$$

The two leaves are also identical in this case (subsystems 2 and 4), these have the properties:

Material: *Gypsum*

$$\text{Dimensions: } 3 * 3 * 0.01m$$

$$E = 4.1 \text{ GPa}$$

$$\vartheta = 0.3$$

$$\rho = 850 \times 0.01 \text{ kg/m}^2$$

$$f_c \approx 2800\text{Hz}$$

The internal loss factor was set to 0.01 for all frequencies and the total loss factor for the plates was estimated to 0.02 (see validation part for single leaf walls). The calculations were made in one-third octave bands with a range of 16-25000Hz. The input power for every one-third octave band was approximately 1.26W.

Equation 3.44 was implemented in the MATLAB code which resulted in that the cavity was modeled as a 2-dimensional subsystem for frequencies below 1.700 Hz above this frequency the cavity is considered as a 3-dimensional subsystem. When developing a model In AutoSEA one must decide if the cavity should be considered as a 2-dimensional or a 3-dimensional subsystem. Because of this, both cases are accounted for. The results are compared and can be found in Figure 5.21-Figure 5.25.

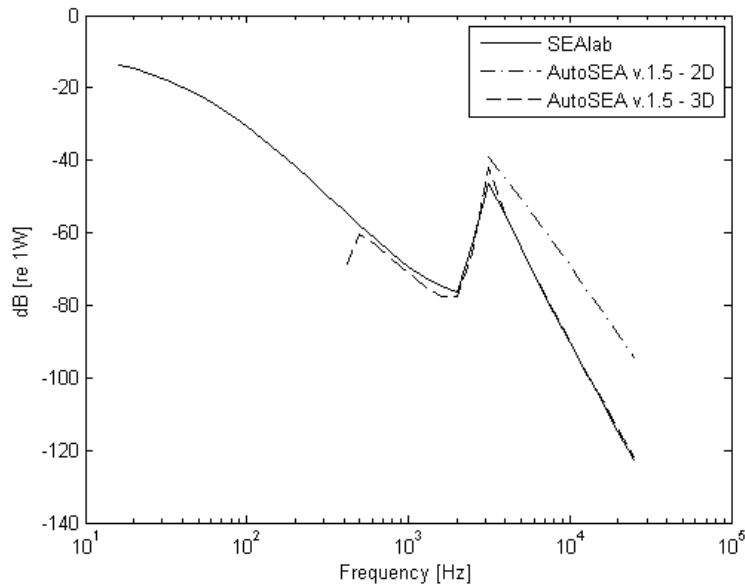


Figure 5.21 Resonant power input from subsystem 4 to subsystem 5 compared to AutoSEA

Figure 5.21 shows the transmitted power from the second leaf (subsystem 4) to the second room (subsystem 5), P_{45} (resonant transmission). AutoSEA does not calculate resonant transmission for frequencies below 400 Hz for the three-dimensional case and 3150 Hz for the two-dimensional. As mentioned before the cavity start acting like a three-dimensional room around 1700 Hz so the resonant path of the two-dimensional case is not of importance here. The correlation between SEAlab and the plot from AutoSEA (3D) are good, especially above 2000 Hz. There is a dip in the AutoSEA result at 400 Hz where the deviation between the two curves is the most.

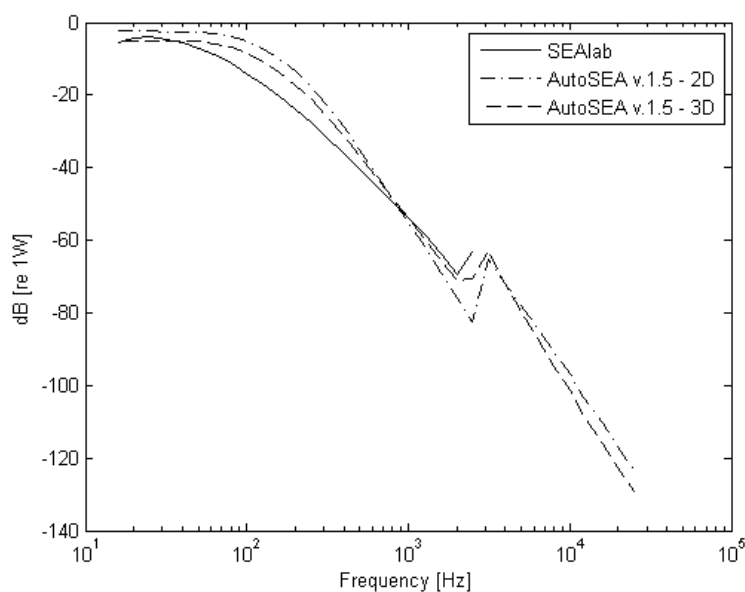


Figure 5.22 Non-resonant input power from subsystem 3 to subsystem 5 compared to AutoSEA

The non resonant power transmission from the cavity to the second room (subsystem 5), P_{35} is presented in Figure 5.22. As can be seen the deviation between the SEALab and AutoSEA results differ more than 3dB for the frequency spans; 40- 630Hz and 1250-1600Hz. For frequencies higher than approximately 1700Hz the cavity acts like a three dimensional room and the correlation becomes better for the 2000 Hz frequency band but the deviation becomes large (7,5 dB) again at the end frequency (2500Hz) of the calculations made by SEALab .

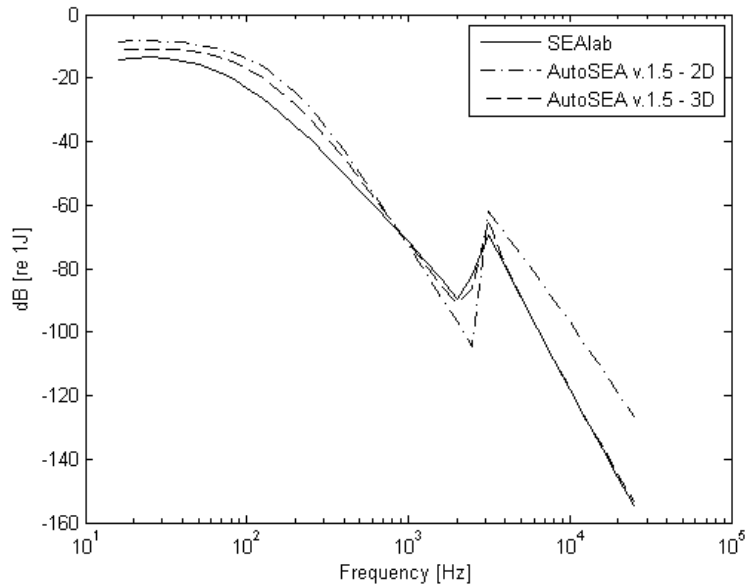


Figure 5.23 Energy subsystem 5 compared to AutoSEA

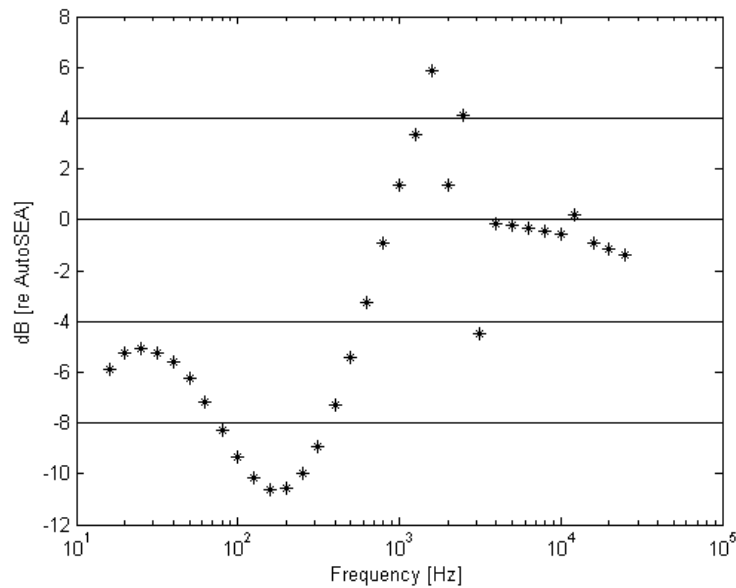


Figure 5.24 Energy of subsystem 5 described as the wave energy in dB from SEALab relative AutoSEA

The total energy in the second room can be seen in Figure 5.23. The difference between the calculations and the results from AutoSEA can then be seen in Figure 5.24 which shows the calculated energy in dB relative the results from AutoSEA. The energy plots confirms the input power results, Figure 5.21 and Figure 5.22, that the main difference is located in the non-resonant energy path with the largest deviation occurring at 160 Hz with a difference of 10.6dB. Above the resonance frequency the results becomes better and in the span of 4000-25000 Hz the largest deviation is below 1.5 dB (25000 Hz).

Instead of total energy the energy in the room can be presented as modal energy, this can be seen in Figure 5.25. The modal energy shows similar behavior as the energy, Figure 5.23.

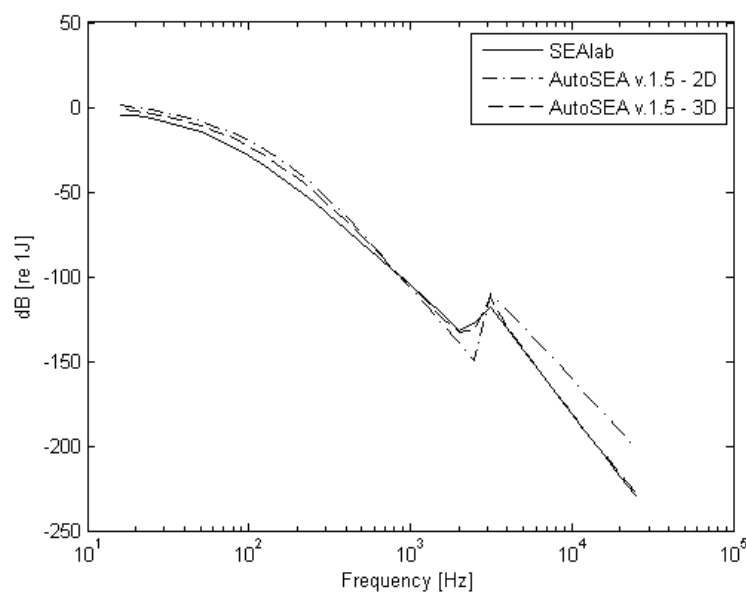


Figure 5.25 Modal energy in subsystem 5 compared to AutoSEA

The properties of the subsystems are identical to the previous example of the single leaf wall. This implies that the validity of the frequency range are the same. The difference is the cavity subsystem which is not present in the single leaf wall case. The cavity fulfills Equation 3.46 for one-third frequency bands above 500 Hz and the upper frequency limit according to Equation 3.53 is identical to the two rooms e.g. 1.600 Hz.

A direct transmission path connecting the two rooms also exists but is not included in the model above due to the incapability of AutoSEA to model this path. The equations used are 4.64-4.71 and the impact of the path can be seen in Figure 5.26.

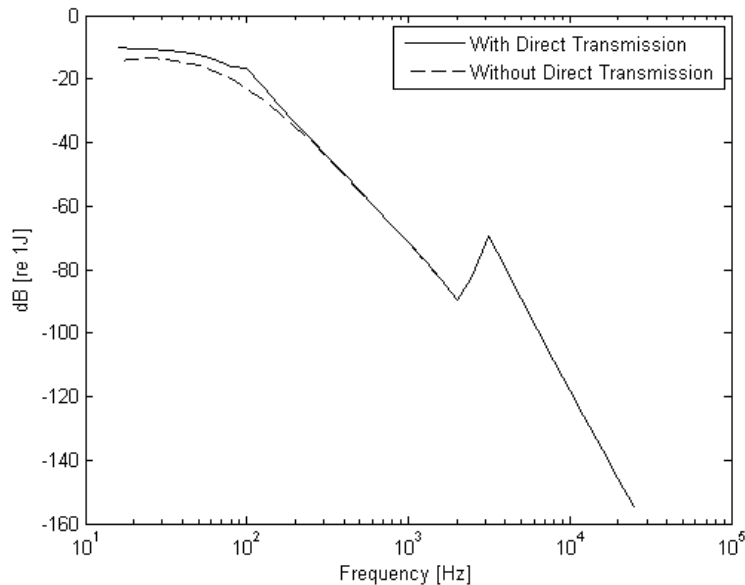


Figure 5.26 Comparison with and without the direct transmission path between room 1 and 2

In Figure 5.26 the addition from the direct path can be seen at the lower frequency region. The largest difference (6.2 dB) in energy level is found at 100Hz. The dip in the plot with the direct transmission path is where the calculations go from modeling the wall as mass-law controlled to spring-stiffness controlled. Above 315 Hz there are barely any contributions from the direct transmission path between room 1 and 2.

The properties of the air cavity stiffness and the important frequencies can be found below:

$$f_{dw} \approx 90\text{Hz}$$

$$f_d \approx 550\text{Hz}$$

$$K = 1387200 \text{ N/m}$$

6 Discussion

The calculations of the structural sound transmission factor correlates well with reference [9] both for the transmission coefficient as a function of incident angle, and for the diffuse transmission coefficient as a function of beam angle, which can be seen in Figure 5.1-Figure 5.4.

The results from the plate-plate transmission are also validated with AutoSEA. One can clearly see that the transmitted bending wave corresponds well with the energy levels obtained from AutoSEA, see Figure 5.5, except for higher frequencies where the worst value differ approximately 0.5dB from AutoSEA data, see Figure 5.6. AutoSEA has unexpected oscillations at high frequencies, which are likely to be erroneous. For the two other wave types, longitudinal and shear, the largest difference is located at the lower frequency bands. The result becomes better compared to AutoSEA with increasing frequency, Figure 5.7 - Figure 5.10. The largest deviation is for transmitted shear wave with 0.7dB at 32Hz compared to AutoSEA, see Figure 5.9. The deviations are due to the limited number of incident angles considered in SEALab when calculating the diffuse field transmission coefficient and the corresponding coupling loss factors.

One can clearly see in Figure 5.11 that the number of incident angles used is not of importance when calculating the transmitted bending wave energy for an incident bending wave case. The results for two other wave types are more dependent on the number of angles used as can be seen in Figure 5.12 and Figure 5.13. By increasing the number of angles the deviation compared to AutoSEA becomes lower, especially for lower frequencies. The drawback by increasing the number of angles is the increase in calculation time.

For sound transmission calculations and for two rooms connected over a single leaf wall the results correlates well overall but with some differences at certain frequencies. Figure 5.15 clearly shows that the resonant path is dominant above the critical frequency 2.800 Hz and corresponds well with the estimation by AutoSEA. The main difference is the lower value of the resonant power transmission AutoSEA gives at 315 Hz and also the higher value at 3.150 Hz. The difference at 3.150 Hz can be explained by the condition in Standard 12354-1, which is implemented in SEALab but not in AutoSEA and states that the radiation efficiency cannot become larger than 2. The deviation located at 315 Hz for the AutoSEA results seems unlikely and erroneous.

The power input into room two by the non-resonant path is dominating the energy flow in the frequency span below 2.500 Hz, Figure 5.16. AutoSEA chooses to calculate a power input for the non-resonant transmission in all frequencies. The calculations made by SEALab do not calculate values above the critical frequency because the calculation method according to standard [4] is not valid in that frequency region. The off-set from the shape of the plot at frequencies over 2.000 Hz is dependent on the total loss factor of the plate. If the total loss factor would be higher than estimated then the curve would have smaller or no off-set, but if it would be less than estimated then the off-

set would be larger and start at a lower frequency. The main level difference in Figure 5.16 occurs at the lowest frequencies. The reason for this is hard to explain except that of discrepancies with the estimations of the non-resonant transmission between AutoSEA and SEALab.

The total energy plot, for subsystem 3, seen in Figure 5.17 corresponds well to the result from AutoSEA with exceptions for some frequencies close to the critical frequency. The results from the SEALab calculations relative the results from AutoSEA is shown in Figure 5.18. In this figure it is even more apparent that the largest deviation occurs close to the critical frequency. The two frequencies that stand out are 2.500 Hz and 3.150 Hz, at these frequencies the results differ over 2dB relative AutoSEA. This is not surprising since the non-resonant power input is much larger at 2.500 Hz than compared to AutoSEA, and as discussed previously this off-set was directly coupled to the total loss factor of the plate. The lower value at 3.150 Hz is directly linked to the fact that according to standard [4] the radiation efficiency is clipped at values above 2, resulting in a lower prediction of the radiation efficiency compared to AutoSEA.

The last figure, Figure 5.19, for the example with a single leaf wall shows the modal energies in the second room (subsystem 3). Here one can see the same behavior as in the total energy plot, Figure 5.17. This shows that the number of modes and modal densities are equivalent to AutoSEA.

As for the case of sound transmission between rooms/cavities separated by two leafs also referred to as a double wall, the resonant power input to subsystem 5 is presented in Figure 5.21. For this case the transmitted energies between the calculated results and those from AutoSEA corresponds well for frequencies above 2.000 Hz, below this frequency there is some deviations. As in the single leaf wall example AutoSEA does not have values for all of the frequency bands, this time the values are zero for frequencies below 400 Hz. The plot where the cavity is treated as a 2-dimensional case is irrelevant since the cavity should be treated as a 3-dimensional room at approximately 1.700 Hz according to equation 3.44. Again a lower estimation of the power input at 3.150 Hz is noticeable and is as mentioned before probably due to the maximum value of the radiation efficiency according to standard 12354-1, which is used in SEALab.

In Figure 5.22 the input power to the second room (subsystem 5) the difference in level is quite large below the critical frequency. The case where the cavity is treated as a 2-dimensional subsystem shall be compared with SEALab up to 1.700 Hz. As can be seen in the figure almost throughout the whole frequency spectrum the results differ, except around 800 Hz. The off-set from the curve path over 2.000 Hz can be seen for the results from SEALab, which were noticed in the previous case as well.

The total energy, as can be seen in Figure 5.23, deviates in the same fashion as the input powers which is reasonable. The decibel values of the ratio between the results from SEALab and AutoSEA, Figure 5.24, clearly shows the large level difference at frequencies below the critical frequency. The results above 3.150 Hz correspond well with AutoSEA. The modal energies again show the

same tendencies as the total energy which is logical since the modal density of each subsystem is calculated in the same way as in the single leaf wall example.

The difference between SEAlab and the AutoSEA software could be a number of things. For example the calculation model for calculating the radiation efficiency and the non-resonant transmission differ and therefore the end result differs. Also the assumptions made in AutoSEA are not fully declared. It is possible that AutoSEA could have some empiric data that is accounted for in the calculations. Another explanation to the difference in result could be that AutoSEA v.1.5 is quite old and the way of calculating radiation efficiency and transmission coefficient has changed since then. SEAlab calculates the radiation efficiency and the transmission coefficients for the non-resonant transmission as standard 12354-1 declares, which can be assumed that AutoSEA v.1.5 does not.

The double wall model does not include the double wall transmission or the transmission from the in-direct plate. The double wall transmission becomes important if the gap between the two leafs are reduced which will send the double wall reduction dip up in frequency. The in-direct transmission is represented by the coupling between a room and the leaf that is the leaf that is furthest away of the two. This transmission becomes an important factor if the two leafs have different characteristics. The result of this is that one will be above resonance frequency earlier than the other resulting in a non-resonant transmission through the non-resonant leaf from the resonant leaf.

The last result, Figure 5.26, is that of the non-resonant path of the double leaf wall from room 1 to room 2. This path is not compared to AutoSEA because the software can only model this transmission path by the mass-law or by user defined properties. The increase in energy levels seen in Figure 5.26 is located in the lower frequency region. The dip in the result at 80Hz is where the software shift from calculating the double wall as a mass controlled to mass-spring-mass controlled system. It is important to keep in mind that the contribution from this path is highly dependent on the width of the cavity. If the width of the cavity is decreased the contribution from this path will increase the energy levels for frequency bands located higher up in frequency.

7 Conclusion

An open source software has been implemented and validated. The software utilizes the theory of Statistical Energy Analysis to calculate the energy transmission between subsystems. The implemented subsystems are plates, rooms and cavities. To calculate the energy transmission among plates connected via a line connection a wave approach has been used. In order to calculate the energy transmission due to area connections between plates and rooms/cavities the radiation efficiency is required. The radiation efficiency is calculated according to standard 12354-1.

It has been shown that SEAlab calculates the structural sound transmission well between two plates coupled along a line connection according to ref [9]. It is also shown that SEAlab correlates well with AutoSEA for plate-plate transmission. The use of 1000 angles as default seem reasonable since it deviates less than 0.1 dB for bending waves, which is the main energy contributor, and at worst 0.7dB at 32Hz for shear waves compared to AutoSEA. One should also keep in mind that there is a rapid increase in calculation time when increasing the number of incident angles.

The sound transmission for the single leaf wall correlated well with the data extracted from AutoSEA. The level difference around the critical frequency can be explained as estimation differences between AutoSEA and standard 12354-1 which is used in SEAlab.

The third example represented by sound transmission through a double-leaf wall needs some improvements in the calculation model. When the calculated results from SEAlab were compared with the results from AutoSEA it showed that the differences in the results from the two software were relatively small above the critical frequency. The problem were at the lower frequencies were the difference was larger. Due to the lack of insight into the commercial software assumptions and calculation process the difference cannot be explained.

The results obtained from the direct path calculation from room 1 to room 2 for the double leaf wall example seems reasonable. The increase is directly linked to the width of the cavity. If the cavity width is decreased then the affect from this path will influence the results at higher frequencies and increase the total energy levels.

In all, we have managed to develop and implement Statistical Energy Analysis with an open source code in MATLAB. The software is able to handle plate-plate transmission and sound transmission between rooms separated by a wall constructed by single or double leaves. SEAlab uses function files to calculate the behavior of a system. The use of functions gives the user a better overview of the software structure and the possibility to change and add functions to fulfill the user's specifications. The user interface can only be used in MATLAB but the calculation functions can be utilized in OCTAVE. With all of this in mind we have successfully manage to fulfill our aim and goal of this Master's thesis.

7.1 Further work

The results from the calculations for the double-leaf wall example did not correlate very well with the results from version 1.5 of AutoSEA for the frequency spectrum below the critical frequency. So as a next step could be to compare SEALab to a more up to date software to be able to determine if the problem lies there. Another validation process could be to compare the simulated values with empirical measured values to determine the accuracy of SEALab. Before the comparison to measured data could be conducted it is probably important to include the non-resonant path from room to room and the indirect power flow from the second plate to the room.

The design of the software enables the user to easily modify or add different types of calculations in form of function files. There are a number of functions that can be added in order to be able to construct more general and complex models. Examples of such functions could be implementations of other types of subsystems such as beams and curved panels. There are also other types of implementations such as including functions for trim, leakage, Wave Intensity Analysis (WIA), etc.

8 References

- [1] Fahy, Frank J. (1994): Statistical energy analysis: a critical overview. *Philosophical Transaction: Physical Sciences and Engineering*, Vol. 346, No. 1681, 1994, pp. 431-447.
- [2] Lyon, Richard H., DeJong Richard G. (1998): *Theory and application of statistical energy analysis*, RH Lyon Corp, Cambridge, {USA/Massachusetts}.
- [3] Craik, Robert J.M. (1996): *Sound transmission through buildings using statistical energy analysis*, Gower, Aldershot, {England/Hampshire}.
- [4] Swedish institute for standards (2000): *SS-EN 12354-1*, SIS, {ICS 91.120.20}, Stockholm, Sweden, 2000.
- [5] Mace, B.R. *Statistical energy analysis*. Four compendiums from Patrik Andersson at the department of applied acoustic, Chalmers University of technology. Gothenburg, Sweden, 2010.
- [6] Plunt, Juha. (1998): *Statistical energy analysis (SEA), Theory and applications*. Course material in the course Technical Acoustics II, Chalmers University of technology. Gothenburg, Sweden, 2010.
- [7] Schönfeld, Stephan. (2008): *Airborne sound transmission loss of a car firewall: Prediction and study using Statistical Energy Analysis*. {Master Thesis}. Department of Civil and Environmental Engineering, 2008:101, Gothenburg, Sweden, 2008.
- [8] Vigran, Tor Erik. (2008): *Building Acoustics*. Taylor & Francis, New York, USA/NY, 2008.
- [9] Langley, R.S., Heron, K.H. (1990): Elastic wave transmission trough plate/beam junctions. *Journal of Sound and Vibration*, Vol. 143, No. 2, December 1990, pp. 241-253.
- [10] Craik, R.J.M., Bosman, C., Cabos, C., Heron, K.H., Sarradj, E., Steel, J.A., Vermeir, G. (2002): Structural transmission at line junctions: a benchmarking exercise. *Journal of Sound and Vibration*, Vol. 272, Issues. 3-5, May 2004, pp. 1086-1096.
- [11] Open source initiative (2010) <http://www.opensource.org/licenses/bsd-license.php>
- [12] Bron-van der Jagt, S. (2007): *Sound transmission through pipe systems and into buildings*. {Ph.D. Thesis}. Technische Universiteit Eindhoven, NUR 950, Eindhoven, The Netherlands, 2007.

Appendix A – Data and folder structure

SEAlab data structure

All variables and data used in SEAlab are stored in a structure array called '*data*'; *data* is stored within the main user interface as application data. This structure array has several levels of structure arrays which will be described in the following section.

The data structure itself has seven field names. These are shown in the tree below, Figure A.1.

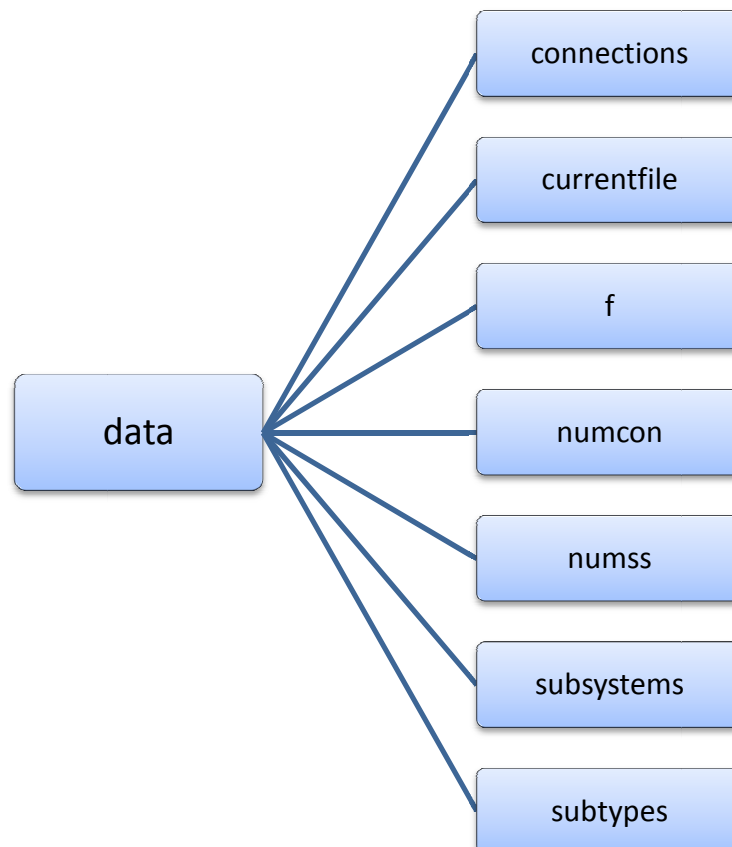


Figure A.1 The substructure of data and its field names

The field names of data can be either a variable or another structure array.

- **connections (structure array).**
The connections structure array holds all variables and data for the connections. If the system have several connections, the first connection is stored in *data.connections(1)*, the second connection in *data.connections(2)* etc. The field names of the connections structure is presented in the following figure.
- **currentfile (string array).**
This is a temporary variable used within the main user interface *mainui.m* to keep track of which file the current workspace is saved to.
- **f (double array).**
Variable that holds the frequencies that the calculations will be made on.

- **numcon (double).**
Variable that holds the number of connections in the system.
- **numss (double).**
Variable that holds the number of subsystems in the system.
- **subsystems (structure array).**
The subsystems structure holds all variables and data for all subsystems. The first subsystem is stored in *data.subsystems(1)*, the second is stored in *data.subsystems(2)* etc. The field names of this structure are presented later in this section.
- **subtypes (structure array).**
A structure array that stores all the names and image data for the different types of subsystems that is available.

Some of the field names for the connections array are also structure arrays. Their field names are presented in the following two trees, Figure A.2 and Figure A.3.

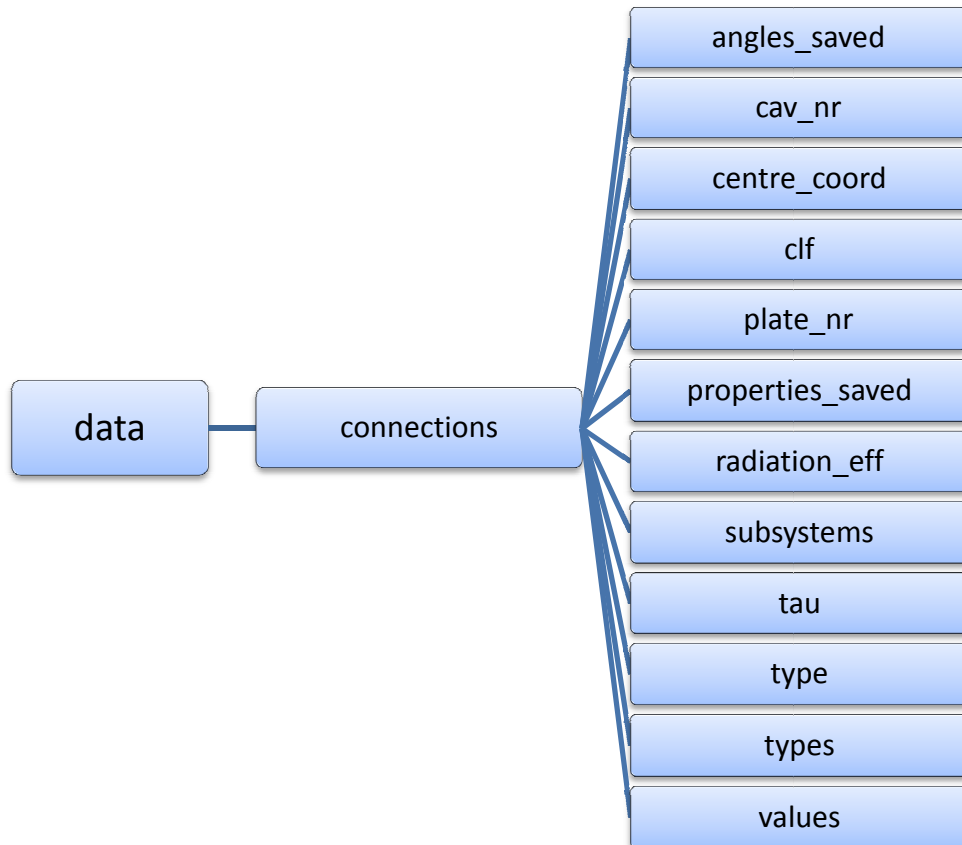


Figure A.2 The substructure of *data.connections* and its field names

- **angles_saved (double).**
Variable that is used if the connection is a line junction with coupled plates. Used by the user interface to check if the user has saved the angles between the coupled plates, 0 if they are not saved and 1 if they are.

- **cav_nr (double array).**
Used for connections between plates and cavities. Cav_nr holds the numbers of the subsystems in the connection that are cavities.
- **centre_coord (double array).**
Variable used by the main user interface *mainui.m* to store the location of the subsystem figures in the workspace.
- **clf (structure array).**
A structure array that stores all coupling loss factors between the subsystems in that coupling. The field names and how this structure array is used are described later in this section.
- **plate_nr (double array).**
Used for connections between plates and cavities. Plate_nr holds the numbers of the subsystems in the connection that are plates.
- **properties_saved (double).**
Variable that is used by the main user interface *mainui.m* to check if all properties are saved for all subsystems before executing the calculations, 0 if the properties are not set and 1 if they are.
- **radiation_eff (structure).**
Radiation_eff is a structure array that stores the radiation efficiency between the plates and the cavities in that connection. Only used for connections between plates and cavities. The field names and how the data is stored are described later in this section.
- **subsystems (double array).**
Variable that holds the numbers of the subsystems in the connection.
- **tau (structure array).**
Tau is a structure array that stores all the transmission coefficients between the subsystems in that coupling. The field names and how this structure array is used are described later in this section.
- **type (string array).**
Variable that describes what type of connection it is.
For example:
A connection of plates coupled over a line junction is called 'plates'.
A connection between one cavity and one plate is called 'plate cavity'.
Two connected cavities and one plate is called 'leaf wall'.
Three connected cavities and two plates is called 'double wall'.
- **types (cell array).**
Types is a cell array where each element is a string array of each subsystem type. For example a single leaf wall connection, the cell array will have three elements with the values: 'cavity', 'plate' and 'cavity' in that order.
- **values (structure array).**
Values is a structure array that holds all properties for the connection. The field names and the properties are described later in this section.

The field names in the structure array *data.connections* that itself are structure arrays have the following field names:

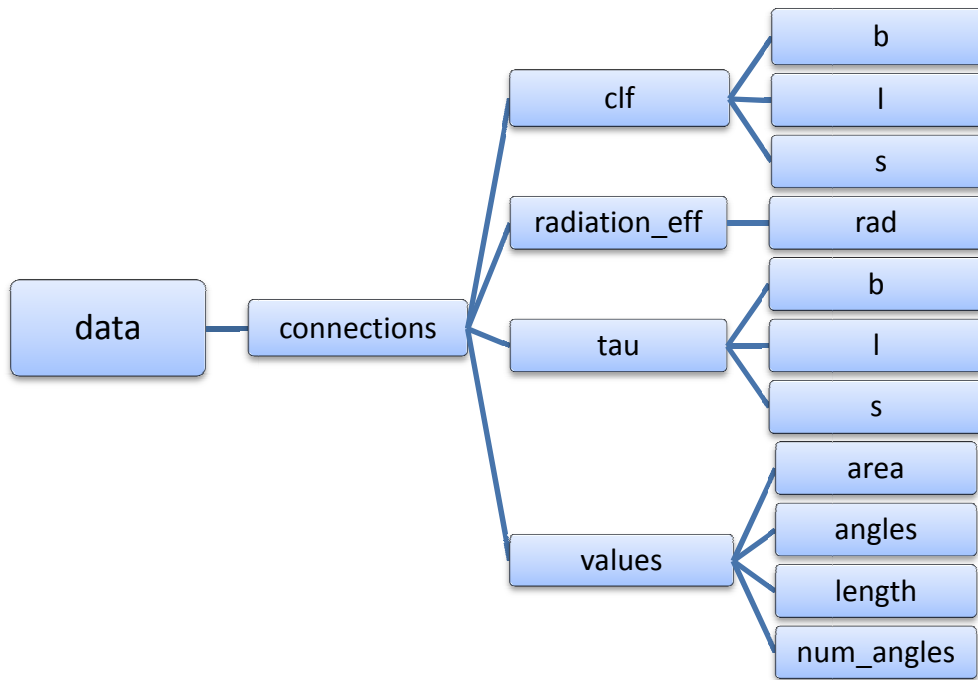


Figure A.3 The substructure of `data.connections` and its field names

- **clf (structure array)**

The coupling loss factor structure array which has been described earlier is three dimensional. If the structure array is described as: $clf(x,y,z)$, then x will represent the subsystem that carries the transmitted energy, y represents the receiving subsystem and z the energy type in the carrying subsystem. z is 1 for bending waves, 2 for longitudinal waves and 3 for shear waves. The type of energy in the receiving subsystem is represented by the field names of the structure array. The field name b represents bending energy, l the longitudinal energy and s the shear energy.

- **b (double array)**

b is a Variable of class double that holds bending energy (over frequency).

- **l (double array)**

l is a Variable of class double that holds longitudinal energy (over frequency).

- **s (double array)**

s is a Variable of class double that holds shear energy (over frequency).

Example:

Two plates (subsystem numbers 4 and 7) are coupled in a connection (connection number one). Subsystem number 4 is the first subsystem in the connection and number 7 is the second subsystem. Longitudinal energy in *subsystem 4* transmitted to shear energy in *subsystem 7* is represented by `data.connections(1).clf(1,2,2).s`.

- **radiation_eff (structure array)**
radiation_eff is a structure array that holds the radiation efficiencies between plates and cavities. If the plate is connected to two cavities, *radiation_eff(1)* holds the radiation efficiency to the first cavity and *radiation_eff(2)* the second. The values are stored in the field name *rad*.
 - **rad (double array)**
 Variable of class double that stores the radiation efficiency.
- **tau (structure array)**
 For coupled plates, the *tau* structure has three dimensions and is used in the same way as the *clf* structure. For more information read the description off the *clf* structure. For coupled plates the field names are also the same as for the *clf* structure.

- **b (double array)**
b is a Variable of class double that holds the transmission coefficient for bending energy (over frequency).
- **l (double array)**
l is a Variable of class double that holds the transmission coefficient for longitudinal energy (over frequency).
- **s (double array)**
s is a Variable of class double that holds the transmission coefficient for shear energy (over frequency).

The *tau* structure is also used for sound transmission between two cavities that are separated by a single leaf wall. In this case *tau* is not three dimensional. For a single leaf wall, *tau(1)* represents the sound transmission with the first cavity as the sending cavity and *tau(2)* with the second cavity as sending. The field names are also different. Since there is only longitudinal energy in cavities (assuming low viscosity), only longitudinal energy transmitted to longitudinal energy in the other cavity is interesting. This sound transmission is represented by the field name *tau*.

- **tau (double array)**
tau is a variable of class double that represents transmitted longitudinal energy to longitudinal energy between two cavities separated by a single leaf wall (over frequency).
- **values (structure array)**
values is a structure array that holds the variables that stores the values that are specific to the specified connection. Depending on the type of connection, the structure array has different field names and values.
 - **area (double)**
area is a variable specific for area connections, such as connections between volumes and plates.
 - **angles (double array)**
 Used for connections between coupled plates. *angles* is a double

array that stores the same amount of angles (in degrees) as there are plates in the connection. The coupling angle between each plate relative the first plate is used. So the first angle in the array is always 0°.

- **length (double)**
Used for line junctions, stores the length of the junction in meters.
- **num_angles (double)**
Used for connections between plates. Stores the amount of incident angles the transmission coefficient between each plate is integrated over.

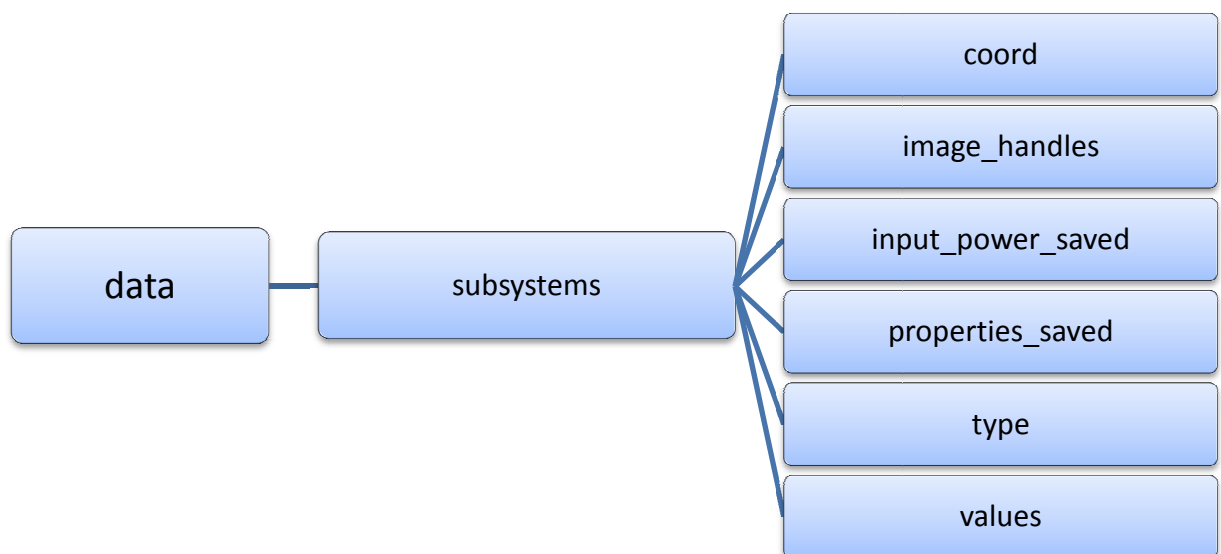


Figure A.4 The substructure of data.subsystems and its field names

- **coord (double array)**
Used by the user interface to store the coordinates for the subsystem figures in the system axes.
- **image_handles (figure handles)**
Stores the figure handles for the subsystem figures in the user interface.
- **input_power_saved (double)**
Used by the user interface to check if the input power is set for the subsystem before starting the calculations.
- **type (string array)**
Stores which type of subsystem it is. Can for example be a string array with: 'plate' or 'cavity'.
- **values (structure array)**
values is a structure array that holds the variables that stores the values that are specific for that subsystem. Depending on the type of subsystem the structure array has different field names and values. The field names are presented in the following figure.

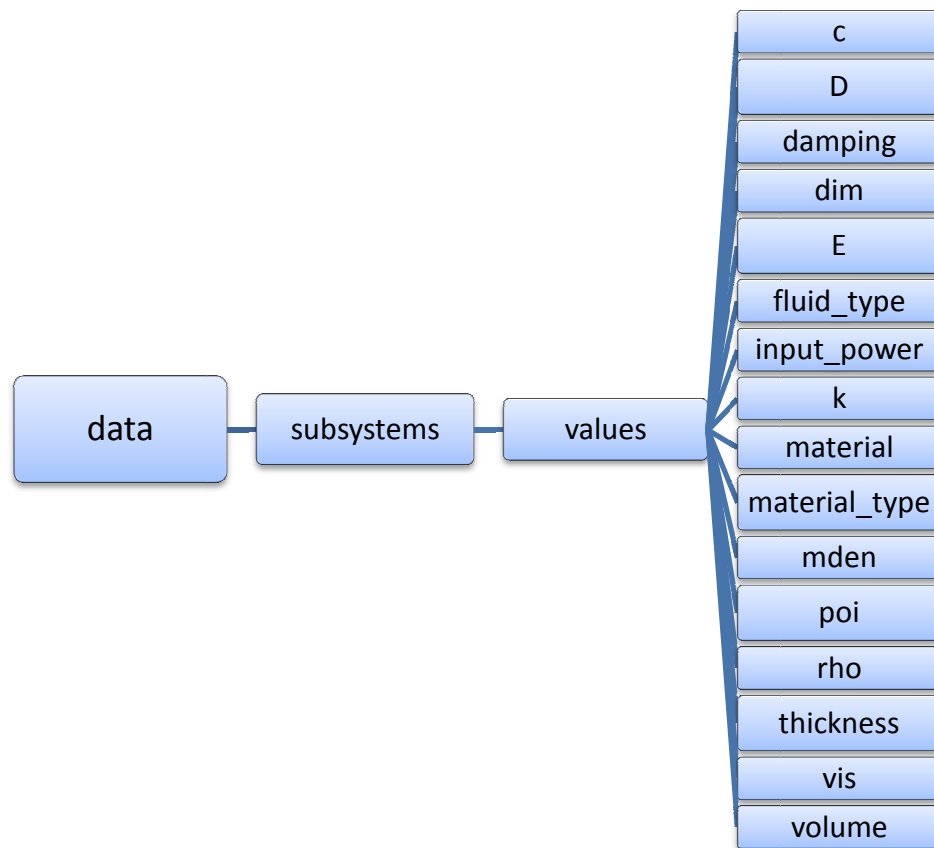


Figure A.5 The substructure of `data.subsystems.values` and its field names

- **c (structure array or double array)**
A variable that depending on the type of subsystem is a structure array or a variable of class: double. If the subsystem is a cavity, *c* is a double array that stores the sound speed in the medium in the cavity (m/s). If the subsystem is a plate, *c* is a structure array that holds the sound speed in the plate for the different wave types treated, which is described further in a later section.
- **D (double)**
Used for plates, stores the bending stiffness of the plate.
- **damping (structure array)**
damping is a structure array that stores the total loss factor of the subsystem, the field names are described in the following figure.
- **dim (double array)**
dim stores the dimensions of the subsystem. Stores two dimensions for plates with the width first and length last. For volumes *dim* stores three dimensions, the width first, height second and the depth of the cavity last (meters).
- **E (double)**
Used for plates and stores the Young's modulus of the plate.
- **fluid_type (string array)**
Used for cavities and semi infinite fluids. *fluid_type* is a string array that

shows the type of fluid in the cavity, for example: 'Air', 'Helium' or 'Water'.

- **input_power (structure array)**
Structure array that stores the input powers to the subsystem, described in the following figure.
- **k (structure array or double array)**
A variable that depending on the type of subsystem is a structure array or a variable of class: double. If the subsystem is a cavity, k is a double array that stores the wave number in the cavity medium. If the subsystem is a plate, k is a structure array that holds the wave numbers in the plate for the different wave types treated, which is described further in the following figure.
- **material (double)**
 $material$ store the location of the type of fluid or material in the .mat file *physicalproperties.mat*.
- **material_type (string array)**
Used for plates. $material_type$ is a string array that shows the type of material the plate is made of. For example: 'Aluminum' or 'Steel'.
- **mden (structure array)**
 $mden$ is a structure array that stores all the modal densities in the subsystem for the different wave types treated.
- **poi (double)**
Used for plates. Poi is a variable that stores the Poisson's ratio for the material of the plate.
- **rho (double)**
 rho is a variable that stores the density of the material or the fluid in the subsystem (kg/m^3).
- **thickness (double)**
Used for plates and stores the thickness of the plate in meters.
- **vis (double)**
Used for cavities and stores the viscosity of the medium in the cavity.
- **volume (double)**
Used for cavities and stores the cavity volume (m^3).

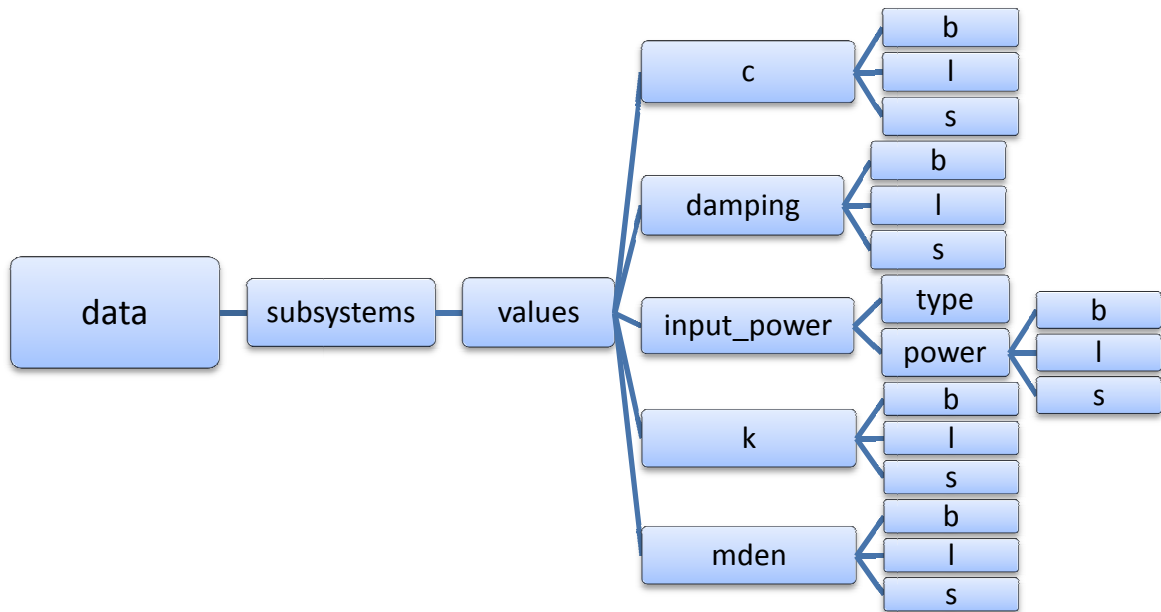


Figure A.6 The substructure of `data.subsystems.values` and its field names

- **c (structure array or double)**
c is a structure array where the wave speed in the subsystem is represented by the different field names. The field name *b* represents bending wave speed, *l* longitudinal wave speed and *s* the wave speed for shear waves.
 - **b (double array)**
b is a Variable of class double that holds bending wave speed (over frequency).
 - **l (double array)**
l is a Variable of class double that holds longitudinal wave speed (over frequency).
 - **s (double array)**
s is a Variable of class double that holds shear wave speed (over frequency).
- **damping (structure array)**
damping is a structure array that holds the total loss factor for the subsystem. The total loss factor for each type of wave is represented by the different field names of the structure. The field name *b* represents the total loss factor for bending waves, *l* for longitudinal waves and *s* for shear waves.
 - **b (double array)**
b is a Variable of class double that holds the total loss factor for bending waves (over frequency).
 - **l (double array)**
l is a Variable of class double that holds the total loss factor for longitudinal waves (over frequency).
 - **s (double array)**
s is a Variable of class double that holds the total loss factor for shear waves (over frequency).

- **input_power (structure array)**
input_power is a structure array for the input powers to the subsystem. It has two field names: *type* and *power*.
 - **type (string array)**
type is a string array that describes what type of excitation the subsystem has. Can for example be: 'Point force, edge', 'Point force, middle' or 'Average'.
 - **power (structure array)**
power is a structure array that holds the input power values for the specific excitation. The power input to the different types of wave energies are represented by the three field names, *b*, *l* and *s*.
 - **b (double array)**
b is a Variable of class double that holds the input power in bending wave energy (in Watt, vector over frequency).
 - **l (double array)**
l is a Variable of class double that holds the input power in longitudinal wave energy (in Watt, vector over frequency).
 - **s (double array)**
s is a Variable of class double that holds the input power in shear wave energy (in Watt, vector over frequency).
- **k (structure array or double)**
k is a structure array that holds the variables that stores the wavenumbers in the subsystem. The different types of waves are represented by the different field names. The field name *b* represents the bending wavenumbers, *l* longitudinal wavenumbers and *s* the wavenumbers for shear waves.
 - **b (double array)**
b is a Variable of class double that holds the bending wavenumber (over frequency).
 - **l (double array)**
l is a Variable of class double that holds the longitudinal wavenumber (over frequency).
 - **s (double array)**
s is a Variable of class double that holds the shear wavenumber (over frequency).
- **mden (structure array)**
The structure array *mden* holds the variables that store the modal densities in the subsystem. The different types of waves are represented by the field names of the structure. The field name *b* represents the modal density for bending waves, *l* for longitudinal waves and *s* for shear waves.
 - **b (double array)**
b is a Variable of class double that holds the bending modal density.

- **l (double array)**
l is a Variable of class double that holds the longitudinal modal density.
- **s (double array)**
s is a Variable of class double that holds the shear modal density.

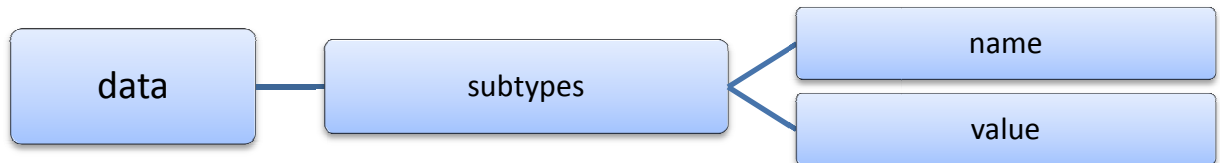


Figure A.7 The substructure of data.subtypes and its field names

- **subtypes (structure array)**
Structure array that stores all the different types of subsystems available to use in the user interface.
 - **name (string array)**
variable that store all the names of the different subsystems (same name as the subsystem figures used in the user interface system). For example: 'plate', or 'cavity'.
 - **values (double array)**
stores the image values of the subsystem figures.

SEAlab folder hierarchy and organization

All files used by SEAlab needs to be structured in folders in order to work. The main folder is called SEAlab which holds a few MATLAB files and some other subfolders, which can be seen in Figure A.8. There are two files in the main SEAlab folder:

- **enablepaths.m**
M-file that is used to add SEAlab subfolders to the MATLAB search paths.
- **SEAlab.m**
The main file to execute from MATLAB to run SEAlab. It will load figures, enable paths, set initial data and start the graphical user interface.

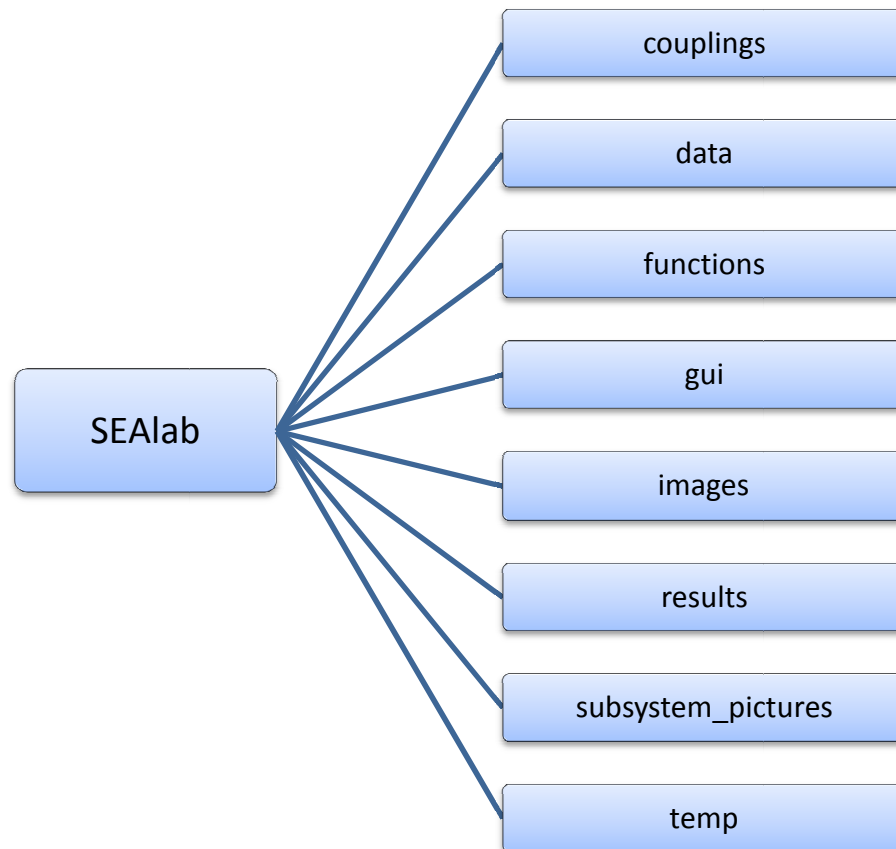


Figure A.8 The folder substructure of SEAlab

The files used in SEAlab is categorized in subfolders:

- **couplings (folder)**
folder for all MATLAB-functions that calculates coupling loss factors, transmission coefficients and radiation efficiencies. The implemented functions are:
 - **clf_double_wall.m**
Function to calculate the coupling loss factors through a double leaf wall.

- **clf_leaf_wall.m**
Function to calculate the coupling loss factors through a single leaf wall.
- **clf_plate_plate.m**
Function to calculate the coupling loss factor between plates coupled over a line junction.
- **clf_plate_roomcav.m**
Function to calculate the coupling loss factor between a plate and a room or cavity.
- **plate_cavity_rad_tau.m**
Function to calculate the radiation efficiency from a plate into a cavity.
- **tau_plate_plate.m**
Function to calculate the transmission coefficients between plates coupled over a line junction.
- **data (folder)**
Folder for all mat-files that stores data and material properties.
Contains the following files:
 - **frequencies.mat**
Mat-file that stores the center frequency values for octave and 1/3-octave bands.
 - **physicalproperties.mat**
Mat-file that stores various material- and fluid properties and data.
- **functions (folder)**
Folder for all other functions used in SEAlab except those that calculates coupling parameters.
 - **calc_c.m**
Function that calculates the wave speed within a certain subsystem.
 - **calc_D.m**
Function that calculates the bending stiffness of a plate.
 - **energy_calc.m**
Function that calculates the energies in each subsystem in a SEA-model.
 - **frequency.m**
Function that calculates and returns a frequency vector of a specified frequency band and frequency range.
 - **loadpicture.m**
Function that reads the images from the subfolder *subsystem_pictures* and returns the values.
 - **mden_calc.m**
Function that calculates the modal densities of plates and cavities.
 - **set_subsystem_values.m**
Function that add and updates fields in the *data.subsystems* structure array.

- **gui (folder)**
Folder for all graphical user interface files used in SEAlab.
 - **excitation.fig and excitation.m**
User interface to set input power and excitation source to a subsystem.
 - **lossui.fig and lossui.m**
User interface to set the total loss factor for a subsystem.
 - **mainui.fig and mainui.m**
The main user interface in SEAlab. Used to create the SEA-modal, set all properties and to start the calculations.
 - **propertiesui.fig and propertiesui.m**
User interface to add/edit or remove material data.
 - **resultsui.fig and resultsui.m**
User interface to see the results from the calculations made in the main user interface.
- **images (folder)**
Folder for all images used in SEAlab (except those for the various subsystems).
 - **long.jpg, point_edge.jpg and point_middle.jpg**
Three images of different excitation sources used in SEAlab.
- **results (folder)**
Folder where the calculated data is saved.
 - **last_data.mat**
The data and results from the latest calculation are stored in *last_data.mat*.
- **subsystem_pictures (folder)**
Folder for the different subsystem types used in SEAlab. Adding a new image of type .jpg to this folder will automatically add the subsystem to SEAlab.
 - **cavity.jpg and plate.jpg**
Images of the three different types of subsystems.
- **temp (folder)**
Folder to store temporary files created by SEAlab.

Appendix B – User guide

The user guide will further explain the features in the interface used in SEALab.

When starting SEALab in MATLAB the main window will appear as can be seen in Figure B.1.

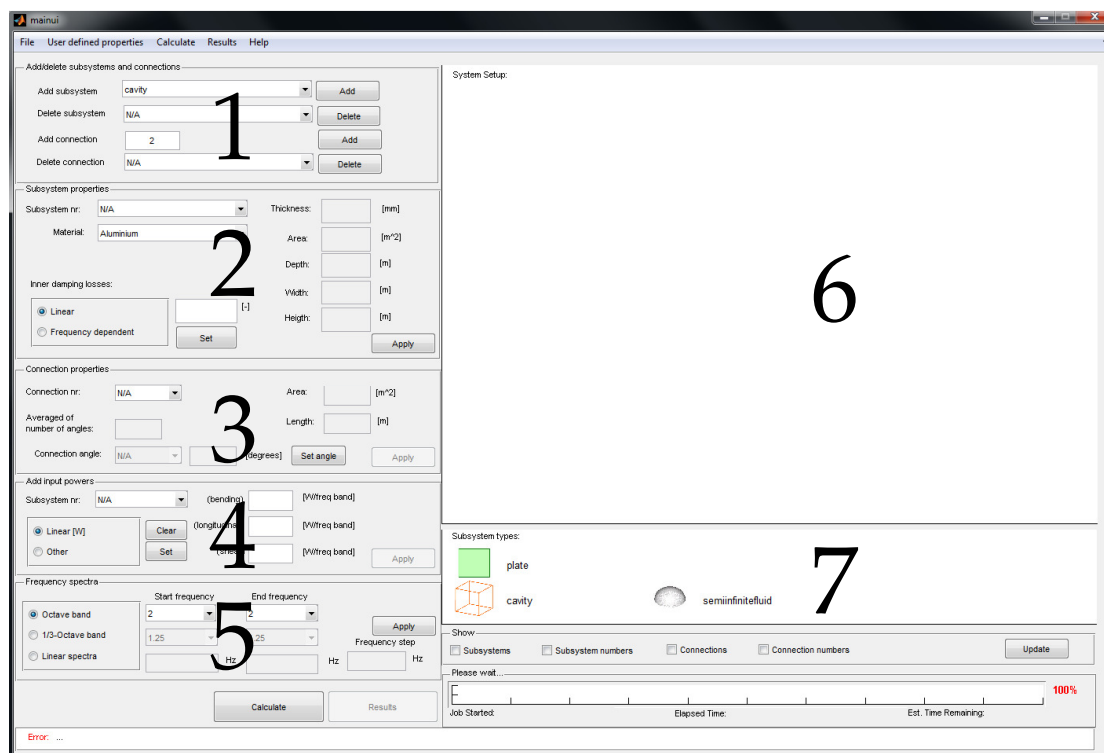


Figure B.1 Main window in SEALab

The different windows 1-5 in the main window are the main setup for typing in the input data and setting the properties of the different subsystems. Window 6 is where the user graphically can see the setup and connections of the system. Window 7 is where the different types of subsystems available are shown as icons.

Window 1

In this window one creates and deletes subsystems and connections. When a subsystem or connection is chosen from window 1 it should be applied in window 6 by clicking on the workspace. Once the user has correctly clicked on window 6 the subsystem or connection applied will graphically appear and be assigned a number to easier keep track of the different connections and subsystems. Currently there are three different types of subsystems that can be added; cavity, plate and semi-infinite fluid. If one wants to connect subsystems with each other one must first decide how many subsystems that should be included in the connection and click add in window 1 and then click on the corresponding number of subsystems in window 6. Note that one must first create the subsystems and *then* create the connections.

Window 2

This window governs the properties of the different subsystems added in window 6. Depending on the subsystem different types of input data will be needed in order for SEAlab to calculate the system. SEAlab detects the kind of subsystem and the needed indata boxes will be enabled. Once all data is typed into the different enabled boxes then click apply for the data to be saved for that particular subsystem. The inner damping losses are set here either as linear or user defined. Note that the frequency span must be set to be able to set the inner damping losses as frequency dependent. When the using the frequency dependent option a new window will appear where the user inputs the data into a table.

Window 3

This window governs the properties of the different connections added in window 6. Depending on the type of connection, line connection or area connection, one needs to add different indata. Similarly to window 2 the indata boxes for the particular connection will be enabled.

Window 4

In this window one chooses the input power for each subsystem. If there is no input power then the value is simply zero. Volumes only have one type of waves and therefore there is only one input power value for the volume. Plates have three different input powers depending on the wave type; bending, longitudinal and shear. The apply button should be applied for every subsystem.

Window 5

Here one chooses the frequency span which the calculations should be made for and the frequency resolution; octave bands, one-third octave bands or user defined as linear spectra with a constant frequency step.

Window 6

This is the work space in SEAlab. Here the user adds subsystems and connections by choosing one in window 1 and then clicking in the work space area. Note that the subsystems are not movable once they are added in the work space. Every subsystem or connection in the workspace is assigned a number. A subsystem or connection is deleted by using the delete option in window 1.

Window 7

In this window the different types of subsystems available are shown as icons. Once the system is feed into the software the system is ready to be calculated and this is done with the calculate button. The calculations are done once the results button appears.

Results

When clicking on the result button a new window will appear: the result window, Figure B.2. The result window contains 5 different areas named window 8-12.

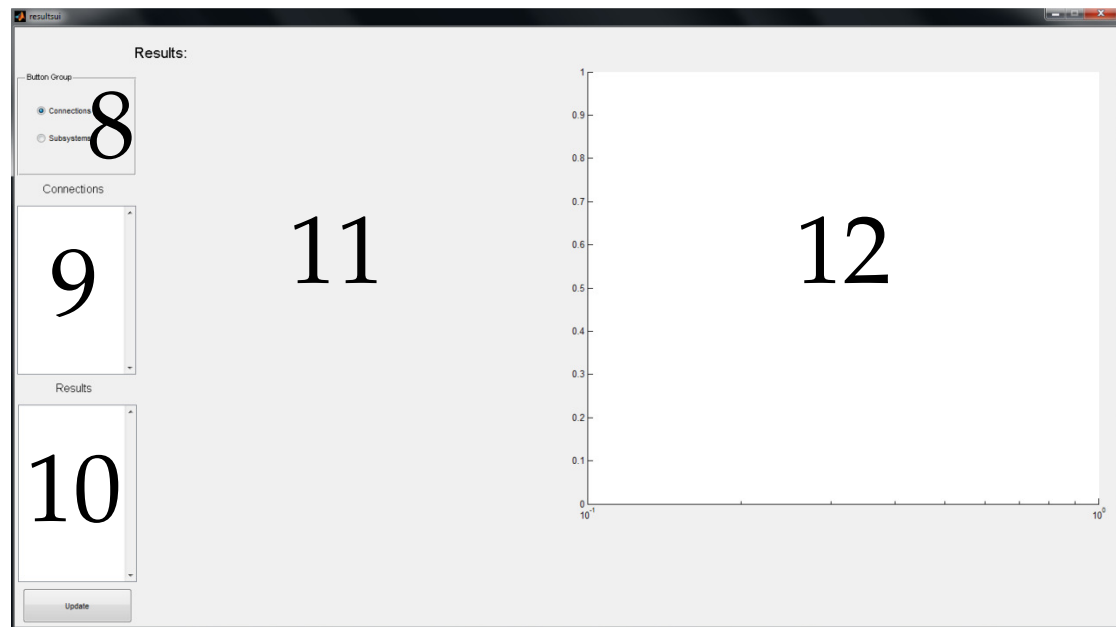


Figure B.2 Result window in SEALab

Window 8

In this window the user first chooses to review the properties and results of the connections or the subsystems.

Window 9

Once the user picks one of the two options in window 8 the different subsystems or connections will appear in this window with its assigned number. Depending on the subsystem or connection there are different results and properties that can be inspected. The available data from the chosen subsystem or connection will be displayed in window 10.

Window 10

The amount of data available in this window depends on the type of subsystem and connection. The data is displayed in window 11 as table and if possible the values are plotted in window 12.

Window 11

Here the result data chosen in window 10 is displayed as tables.

Window 12

Here the result data chosen in window 10 is displayed as plots if possible.

There are three main setups implemented in SEALab; plate-plate transmission and area transmission between rooms separated by a single or double leaf wall. In the following a short tutorial on how to implement the different connection types will be described.

Plate-Plate: The setup is to create the number of plates needed and then create the connection corresponding to the number of plates included in the junction. In Figure B.3 a simple transmission between two plates are shown.

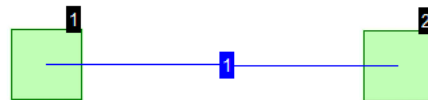


Figure B.3 SEALab schematics of two plates connected via a line junction

Single leaf wall: In this setup one must first create two cavities and one plate. Then a three subsystem connection should be applied as can be seen in Figure B.4 below. When all of the properties are applied the system can be calculated. When using this setup the resonant and non-resonant paths are included.

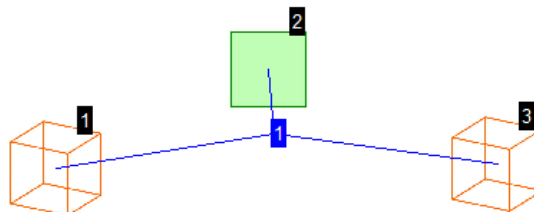


Figure B.4 SEALab schematics of single leaf wall transmission

Double leaf wall: This system requires three cavities and two plates. Once the subsystems are created a five subsystem connection should be applied as can be seen in Figure B.5 below. When using this setup the resonant and non-resonant paths are included in the calculations.

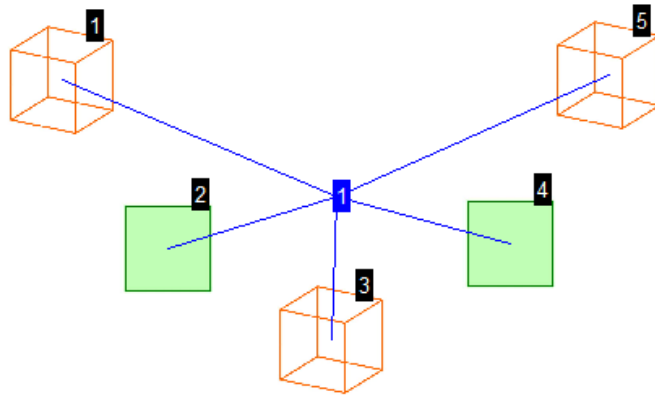


Figure B.5 SEAlab schematics of double leaf wall transmission